General Disclaimer

One or more of the Following Statements may affect this Document

- This document has been reproduced from the best copy furnished by the organizational source. It is being released in the interest of making available as much information as possible.

- This document may contain data, which exceeds the sheet parameters. It was furnished in this condition by the organizational source and is the best copy available.

- This document may contain tone-on-tone or color graphs, charts and/or pictures, which have been reproduced in black and white.

- This document is paginated as submitted by the original source.

- Portions of this document are not fully legible due to the historical nature of some of the material. However, it is the best reproduction available from the original submission.

Battelle
Columbus Laboratories

Report

FINAL PROGRESS REPORT

on

QUANTUM CHEMICAL CALCULATION OF THE EQUILIBRIUM STRUCTURES OF SMALL METAL ATOM CLUSTERS

to

NATIONAL AERONAUTICS AND SPACE ADMINISTRATION
AMES RESEARCH CENTER

August 11, 1982

by

Luis R. Kahn

Grant NSG-2027

BATTELLE
Columbus Laboratories
505 King Avenue
Columbus, Ohio 43201

EXECUTIVE SUMMARY

Clusters of metal atoms are of importance as models of substrates in studies of Chemisorption on metal surfaces and of catalysis of chemical reactions; they are also of increasing interest as novel molecular species in their own right that, surrounded by certain ligands, are possibly a whole new class of catalysts. Moreover, clusters of metal atoms are useful as prototype atomic-level host systems for the development and testing of models on interatomic forces. These interatomic forces are a basic ingredient to the much more complex atomic modeling of the mechanical properties of metals that are used to address important materials problems such as the effect of hydrogen on crack propagation.

The approach we have taken to the study of metal atom clusters is based on the application of ab initio quantum mechanical approaches. This final report discusses our current research effort in the application of these methods. Because these large "molecular" systems pose special practical computational problems in the application of the quantum mechanical methods, there is a special need to find simplifying techniques that do not compromise the reliability of the calculations. Our current research is therefore directed towards various aspects of the implementation of the Effective Core Potential (ECP) technique for the removal of the metal atom core electrons from the calculations. This final report discusses our recent progress in this area.

QUANTUM CHEMICAL CALCULATION OF THE EQUILIBRIUM STRUCTURES OF SMALL METAL ATOM CLUSTERS

by

Luis R. Kahn

INTRODUCTION

The goal of this research is to gain quantitative fundamental understanding about the properties of clusters of metal atoms. The increasing interest in these novel "molecular" species stems from their use to model substrates in the study of chemisorption, and from the prospects that such studies will yield the long-sought understanding of the mechanisms of heterogeneous catalysis of chemical reactions. Moreover, these metal atom clusters surrounded by carbonyl groups, are indeed being thought of as new types of catalysts in their own right. In every case, however, there is still very little known yet about these interesting new molecular species. Since the atomic level properties of these clusters are not yet readily available from experiment, the most reliable approach to their determination lies in the development and application of predictive ab initio quantum mechanical approaches.

This final report describes our current research effort designed to continue the development of a reliable, more accurate, and more efficient quantum mechanical method necessary for the calculation of the properties of clusters of metal atoms. The method deals with the important simplification in the quantum mechanical calculation of metal atom clusters of the removal of the metal atom core electrons from the calculations. The method is the Effective Core Potential (ECP) approach to simulate the effect of the core electrons on the valence electrons.[1]

SCIENTIFIC PROGRESS

A New Theoretical Analysis of the ECP Method

A long standing issue in the Approach of Effective Core Potentials (ECP's) has been the absence of a theoretical analysis on the basis of which

the properties of the ECP's could systematically be improved, a theoretical analysis that would unify the evolving but seemingly disparate proposed improvements to the approach. We have succeeded in finding this needed unifying theoretical analysis for the ECP approach, and a paper describing this work will be appearing in the International Journal of Quantum Chemistry.[2] A preprint of this paper is found in Appendix A of this final report.

We summarize here the background to this theoretical development. As is well known, the first ECP's were based on valence pseudo-orbitals constructed from linear combinations of atomic orbitals of the same orbital angular momentum. While these first ECP's led to some excellent comparisons with molecular all electron calculations, they also led to some perplexing failures. An ad-hoc remedy was proposed by Hay et al,[3] based on the discovery of the sensitivity of the molecular potential energy curves to the long-range properties of the ECP's. Whereas the ad-hoc remedy was found to lead to molecular potential energy curves that were in much better agreement with all electron results, a fundamental explanation was lacking. A fundamental understanding of the problem was found in the recognition of the charge redistribution that was unwittingly being introduced in the valence pseudo-orbitals by the linear-combination-of-atomic-orbitals aspect of its definition. The improper long-range behavior of the ECP's was in retrospect only a symptom of this more fundamental deficiency in the valence pseudo-orbitals. The result has been the development of the "shape consistent" valence pseudo-orbitals. Whereas it appears that a number of workers discussed this idea.[4-8] Christiansen et al[6] were the first to demonstrate the important implications of "shape consistency" for the reliable calculation of molecular potential energy curves. Moreover, the practical procedures of the Christiansen et al approach for the construction of "shape" consistent" valence pseudo-orbitals appear to be the most widely adopted presently.

Notwithstanding the practical success of the "shape consistent" approach, a common concern has been not only that the core segment of the valence pseudo-orbital is arbitrary except for the single condition of normalization, but that no physical criteria had been established to decide even in principle just what additional conditions the core segment of the valence pseudo-orbital should satisfy. This concern has been heightened by the observation in practice of unexpectedly sharp spatial characteristics

in the "shape consistent" ECP's. In the absence of a comprehensive theoretical analysis it has been difficult to decide whether these properties of the ECP are physically important properties or merely artifacts of the insufficient physical definition of the core segment of the valence pseudo-orbital.

Through the valence pseudo-orbitals and the ECP one is, of course, attempting to simulate as closely as possible the parent atomic all-electron Hartree-Fock solution. Indeed, Rappé et al[9] have proposed that the core segment of the valence pseudo-orbital also be required to minimize the error in the valence-valence interactions. Their approach, named the "hamiltonian and shape consistent" approach, points to an important additional physical criterion on the basis of which to remove some of the arbitrariness left in the definition of the core segment of the valence pseudo-orbitals. The minimization of the valence-valence interactions is a global property of the orbitals and, notwithstanding its importance, is a quite disparate property of the parent all electron Hartree-Fock orbitals than the normalization condition. Moreover, the details of the valence-valence interactions are closely dependent on the particular electronic state, and change from one atom to the next in a complicated manner.

Our solution to these important issues in the ECP approach is described in detail in Appendix A. We point out here the main properties and conclusions of this novel development.[2]

(1) A new set of attributes of the atomic orbitals is found that alone determine the valence-valence interactions fully. These new physical measures of orbital characteristics are found in the "moment accumulation" functions defined as

$$Q^{\lambda}_{n\ell,n'\ell'}(r) \equiv \int_0^r P_{n\ell}(t)\, t^{\lambda}\, P_{n'\ell'}(t)\, dt \quad , \; 0 \le r < \infty$$

where $P_{n\ell}$ and $P_{n'\ell'}$ are atomic radial functions.

(2) Since these "moment accumulation" functions determine the valence-valence interactions, the minimization of the error in these orbital properties in turn minimizes the error in the valence-valence interactions.

The latter is shown to be equivalent to the requirement that the core segment of the the valence pseudo-orbital satisfy the conditions

$$\left\{ \tilde{Q}^{\lambda}_{n\ell,n'\ell'}(r_M) = Q^{\lambda}_{n\ell,n'\ell'}(r_M) \; ; \; \lambda = |\ell-\ell'|, \ell+\ell', 2 \; ; \; n\ell \in \underset{\sim}{V} \; ; \; n'\ell' \in \underset{\sim}{V} \right\}$$

The point at which the core and valence segments of the valence pseudo-orbital are joined is denoted as r_M In the above, the superscript tilde indicates the terms constructed from valence pseudo-orbitals rather than the parent valence Hartree-Fock orbitals. The set of valence orbitals is denoted as $\underset{\sim}{V}$.

(3) The previous sole requirement of normalization is found now to be only one of the new conditions. The new requirements, however, are also shown to be discrete individual conditions on the orbitals of the same succint nature as the normalization condition. Since the satisfaction of these conditions minimizes the error in the valence-valence interactions, the "Hamiltonian and shape consistent" condition is, through these conditions, shown in fact not to be a disparate set of conditions from the normalization condition. Moreover, the satisfaction of the "Hamiltonian and shape consistent" condition is hereby extricated from the complexities of the state dependent atomic energy expressions.

(4) Indeed, it is possible to extend the required set of conditions systematically to attain an ever increasing simulation of the orbital characteristics (that, in turn, determine the interactions among electrons) without being limited by the difficulties of finding some pertinent model energy expression. There is, of course, a limit to such a generalization imposed by our overriding goal to project out core states through the requirement of nodelessness in the valence pseudo-orbital, as well as our practical requirement of obtaining valence pseudo-orbitals that are "smooth" over the core region.

(5) A novel expression for the ECP is obtained in terms of the "moment accumulation" functions that allows us to prove that the residual in the valence-valence interactions strictly vanishes for $r \geq r_M$ if the valence pseudo-orbital satisfies the "hamiltonian and shape consistent" conditions. This explains in large measure the extremely sharp behavior already observed in "shape consistent" ECP's around $r \approx r_M$. Whereas the residual in the valence-valence interactions is present for $r < r_M$, the residual is forced to vanish for $r \geq r_M$ by virtue of the conditions built into the core-segment of the valence pseudo-orbital. This effect takes place at whatever value r_M is given, and, therefore, explains the observed change in the shape of the ECP's with changes of r_M.

In summary, this new theoretical analysis yields understanding of previously observed yet unexplained properties of the "shape consistent" ECP's, it unifies the previous "shape consistent" approach with the more recent "shape and hamiltonian consistent" approach, it shows that the orbital attributes that control the valence energy are the "moment accumulation" functions, it affords an analysis of the long-range behavior of the ECP in terms of the "moment accumulation" function, and it provides a foundation for the future construction of systematically improved ECP's.

Evaluation of Matrix Elements of the ECP

In the semiannual progress report of October 23, 1981, we presented the reformulation of the integrals over cartesian gaussian basis functions (GTO) of the molecular ECP so that the shell structure of the GTO's could be exploited. A computer program that yields all the terms in these formulae shell by shell has been prepared and a copy is given in Appendix B. This program yields all the unique non-zero terms, and is thus the replacement for the ENCODER routines of the current SPDF ECP integral program. The other major input to these formulae are the radial integrals, $I_{n,\ell}$ and $J_{n;\ell,\ell'}$. The routines that calculate these latter integrals are the same ones that are already present in the current SPDF ECP integral program.

Whereas the calculation of the ECP integrals over shells is likely to yield a large computational savings, there are other efforts under way by workers at the National Bureau of Standards that have promise to improve the efficiency of the evaluation of the radial $I_{n,\ell}$ and $J_{n;e,e'}$ integrals. This work aims at the direct numerical calculation of the integrals over the ECP on a grid of points. This approach may find advantages in the interchange of the sum over terms with the sum over quadrature points. Another goal of the latter work is to bypass the step of fitting the numerical ECP with GTO's. This step has become one of increased difficulty as a result of the very sharp approach to zero of the "shape consistent" ECP's as r approaches r_M; this property of the ECP can be expected to remain in the "hamiltonian and shape consistent" approach on the basis of the analysis presented above in terms of the "moment accumulation" functions.

There remain, thus, well defined technical problems in the implementation of various ideas for the improved efficiency of the ECP integral calculation. The prospects are good, however, that these will be solved, and that thereby the use of the ECP approach will be extended from a research tool to a bonafide "engineering" tool for chemical research.

REFERENCES

1. L. R. Kahn and W. A. Goddard, Chem. Phys. Lett, 2, 667 (1968); J. Chem. Phys., 56, 2685 (1972). C. F. Melius, W. A. Goddard, and L. R. Kahn, J. Chem. Phys., 56, 3342 (1972). L. R. Kahn, P. Baybutt, and D. G. Truhlar, J. Chem. Phys., 65, 3826 (1976). R. N. Euwema, and L. R. Kahn, J. Chem. Phys., 66, 306 (1977). P. J. Hay, W. R. Wadt, and L. R. Kahn, J. Chem. Phys., 68, 3059 (1978). L. R. Kahn, P. J. Hay, and R. D. Cowan, J. Chem. Phys., 68, 2386 (1978). W. R. Wadt, P. J. Hay, and L. R. Kahn, J. Chem. Phys., 68, 1752 (1978). P. Baybutt, F. W. Bobrowicz, L. R. Kahn, and D. G. Truhlar, J. Chem. Phys., 68, 4809 (1978). P. J. Hay, W. R. Wadt, L. R. Kahn, and F. W. Bobrowicz, J. Chem. Phys., 69, 984 (1978). P. J. Hay, W. R. Wadt, L. R. Kahn, R. C. Raffenetti, and D. H. Phillips, J. Chem. Phys., 71, 1767 (1979); N. H. Sabelli, L. R. Kahn, and R. Benedek, J. Chem. Phys., 73, 6259 (1980); R. J. Bartlett, L. R. Kahn, and G. D. Purvis, J. Chem. Phys., 76, 731 (1982).

2. Also, Luis R. Kahn, "The Effective Core Potential Method and the Calculation of Potential Surfaces by Treating the Valence Electrons Only", NRCC Workshop on Effective Potentials, held at Los Alamos National Laboratory, June 15-17, 1981; and, Luis R. Kahn, "Electronic Structure of Molecules Using One-Component Wavefunctions and Relativistic Effective Core Potentials", International Symposium on "Relativistic Effects in Quantum Chemistry", held at Abo Akademi, Turku, Finland, June 20-23, 1982.

3. P. J. Hay, W. R. Wadt, and L. R. Kahn, J. Chem. Phys., 68, 3059 (1978).

4. Ph. Durand and J. C. Barthelat, Theoret. Chim. Acta 38, 283 (1975).

5. A. Redondo, W. A. Goddard, III, and T. C. McGill, Phys. Rev. B 15, 5038 (1977).

6. D. Christiansen, Y. S. Lee, and K. S. Pitzer, J. Chem. Phys. 71, 4495 (1979).

7. D. R. Hamann, M. Schluter, and C. Chiang, Phys. Rev. Lett. 43, 1494 (1979).

8. A. Zunger, J. Vac. Sci. Tech. 16, 1337 (1979).

9. A. K. Rappé, T. A. Smedley, and W. A. Goddard, III, J. Phys. Chem. 85, 1662 (1981).

APPENDIX A

RELATIVISTIC ELECTRONIC STRUCTURE OF MOLECULES USING ONE COMPONENT WAVEFUNCTION AND RELATIVISTIC EFFECTIVE CORE POTENTIALS

ELECTRONIC STRUCTURE OF MOLECULES USING ONE-COMPONENT WAVEFUNCTIONS AND RELATIVISTIC EFFECTIVE CORE POTENTIALS

Luis R. Kahn

Battelle's Columbus Division
505 King Avenue
Columbus, Ohio 43201 USA

Submitted for publication in the International Journal of Quantum Chemistry, Proceedings of the International Symposium of "Relativistic Effects in Quantum Chemistry", Turku, Finland, June 20-23, 1982.

ELECTRONIC STRUCTURE OF MOLECULES USING ONE-COMPONENT WAVEFUNCTIONS AND RELATIVISTIC EFFECTIVE CORE POTENTIALS

Luis R. Kahn

Battelle's Columbus Division
505 King Avenue
Columbus, Ohio 43201 USA

ABSTRACT

A one-component approach to molecular electronic structure is discussed that includes the dominant relativistic effects on valence electrons and yet allows the use of the traditional quantum chemistry techniques. The approach starts with one-component Cowan-Griffin relativistic orbitals that successfully incorporate the effects of the mass-velocity and Darwin terms present in more complicated wavefunctions such as the Dirac-Hartree-Fock. The approach then constructs "relativistic" effective core potentials (RECP's) from these orbitals, and uses these to bring the relativistic effects into the molecular electronic calculations. The use of effective 1-electron spin-orbit operators in conjunction with these one-component wavefunctions to include the effects of spin-orbit coupling is discussed. Applications to molecular systems involving heavy atoms and comparisons with available spectroscopic data on molecular geometries and excitation energies is presented. Finally, a new approach to the construction of RECP's encompassing the Hamiltonian and shape consistent approach is presented together with a novel analysis of the long-range behavior of the RECP's.

1. INTRODUCTION

This paper reviews various aspects of a practical but nontraditional approach to molecular relativistic electronic structure calculations. Whereas it is traditional to approach relativistic electronic structure in terms of four-component[1-3], or even two-component[4,5], wavefunctions, the present approach is based on one-component wavefunctions familiar from the nonrelativistic theory. It appears, moreover, that the relativistic contributions to molecular properties of chemical interest are being reliably calculated in all cases examined by this approach despite the approximations from which the simplicity of the approach derives.

2. APPROACH

This one-component approach to molecular relativistic electronic structure calculations has two basic ingredients. These are:

(1) One-component Cowan-Griffin relativistic atomic orbitals[6]

(2) "Relativistic" effective core potentials[7].

We review the essential properties of these two ingredients to the present approach next.

2.1 Relativistic Atomic Orbitals

The one-component relativistic atomic orbitals that are the basis of this approach are obtained from the Cowan-Griffin equations.[6] The

latter may be derived qualitatively from the local potential approximation to the Dirac-Hartree-Fock equations

$$P_K' = -\frac{K}{r} P_K + \frac{\alpha}{2}\left[\epsilon - V(r) + \frac{4}{\alpha^2}\right] Q_K \qquad (1)$$

$$Q_K' = \frac{\alpha}{2}\left[V(r) - \epsilon\right] P_K + \frac{K}{r} Q_K \qquad (2)$$

where P_K and Q_K are the "large" and "small" components, respectively, where $\alpha = 1/137.036$ is the fine-structure constant, and where

$$K = \ell \qquad \text{if} \qquad j = \ell - \tfrac{1}{2} \qquad (3)$$

$$K = -\ell - 1 \qquad \text{if} \qquad j = \ell + \tfrac{1}{2} \qquad (4)$$

Solving Equation (1) for Q_K and Q_K', inserting these in Equation (2), and averaging the explicitly j-dependent K term,

$$\bar{K} = \frac{1}{2\ell+1} \sum_{j=\ell-\frac{1}{2}}^{\ell+\frac{1}{2}} (2j+1)\, K = -1 \qquad (5)$$

one obtains an equation that in its form is the Cowan-Griffin equation. The actual Cowan-Griffin, or relativistic Hartree-Fock (RHF), equation is

$$\left[H_{NR} + H_{MV} + H_D \right] P_{n\ell}(r) = \epsilon_{n\ell} P_{n\ell}(r) \tag{6}$$

where H_{NR} contains the non-relativistic terms found in the Hartree-Fock equation,

$$H_{NR} = -\frac{1}{2}\frac{d^2}{dr^2} + \frac{\ell(\ell+1)}{2r^2} + V_{n\ell} \tag{7}$$

whereas H_{MV} and H_D are the relativistic terms known as the mass-velocity and Darwin terms, respectively,

$$H_{MV} = -\frac{\alpha^2}{2}\left[\epsilon_{n\ell} - \bar{V}_{n\ell}(r) \right]^2 \tag{8}$$

$$H_D = -\frac{\alpha^2}{4}\delta_{\ell,0}\left[1 + \frac{\alpha^2}{2}\left[\epsilon_{n\ell} - \bar{V}_{n\ell}(r) \right] \right]^{-1} \frac{d\bar{V}_{n\ell}}{dr}\left(\frac{d}{dr} - \frac{1}{r} \right) \tag{9}$$

The potential $V_{n\ell}$ in Equation (7) contains the usual nonlocal Hartree-Fock potential. However, the analogous potential in Equations (8) and (9) is replaced by a "local exchange" potential,[6,8] $\bar{V}_{n\ell}(r)$.

The atomic orbitals obtained from the RHF equation show the typical qualitative contraction of low ℓ quantum number orbitals and the expansion of the high ℓ quantum number orbitals when compared to the non-relativistic orbitals. This is illustrated in Figures 1 and 2 where the comparisons are for the 7s and 5f orbitals of Uranium atoms, respectively. One also finds good quantitative agreement between the orbital properties obtained from the average of Dirac-Hartree-Fock (DHF) and RHF orbitals. This is illustrated in Table 1 for both orbital radial characteristics and orbital energies in the Uranium atom. Moreover, virtually identical excitation energies are shown in Table 2 for the DHF and RHF calculations on the Au atom, whereas the nonrelativistic results predict even the incorrect ordering of the states for the $5d \rightarrow 6s$ and $6s \rightarrow 6p$ transitions.

2.2. "Relativistic" Effective Core Potentials

The second ingredient to the approach is the use of Effective Core Potentials (ECP's) to bring the relativistic effects on the valence electrons from the atomic calculations into the molecular calculations. The ECP approach was first developed to serve as a device to bring into a molecular calculation the effects onto the valence electrons of the chemically inert core electrons. Since the sources of the relativistic direct and indirect effects on the valence electrons also are localized about the atomic nucleus, the role of the ECP's was expanded to bring the relativistic effects from the atomic calculations into the molecular calculations as well. In this expanded role the ECP became an "relativistic" ECP or RECP.[7]

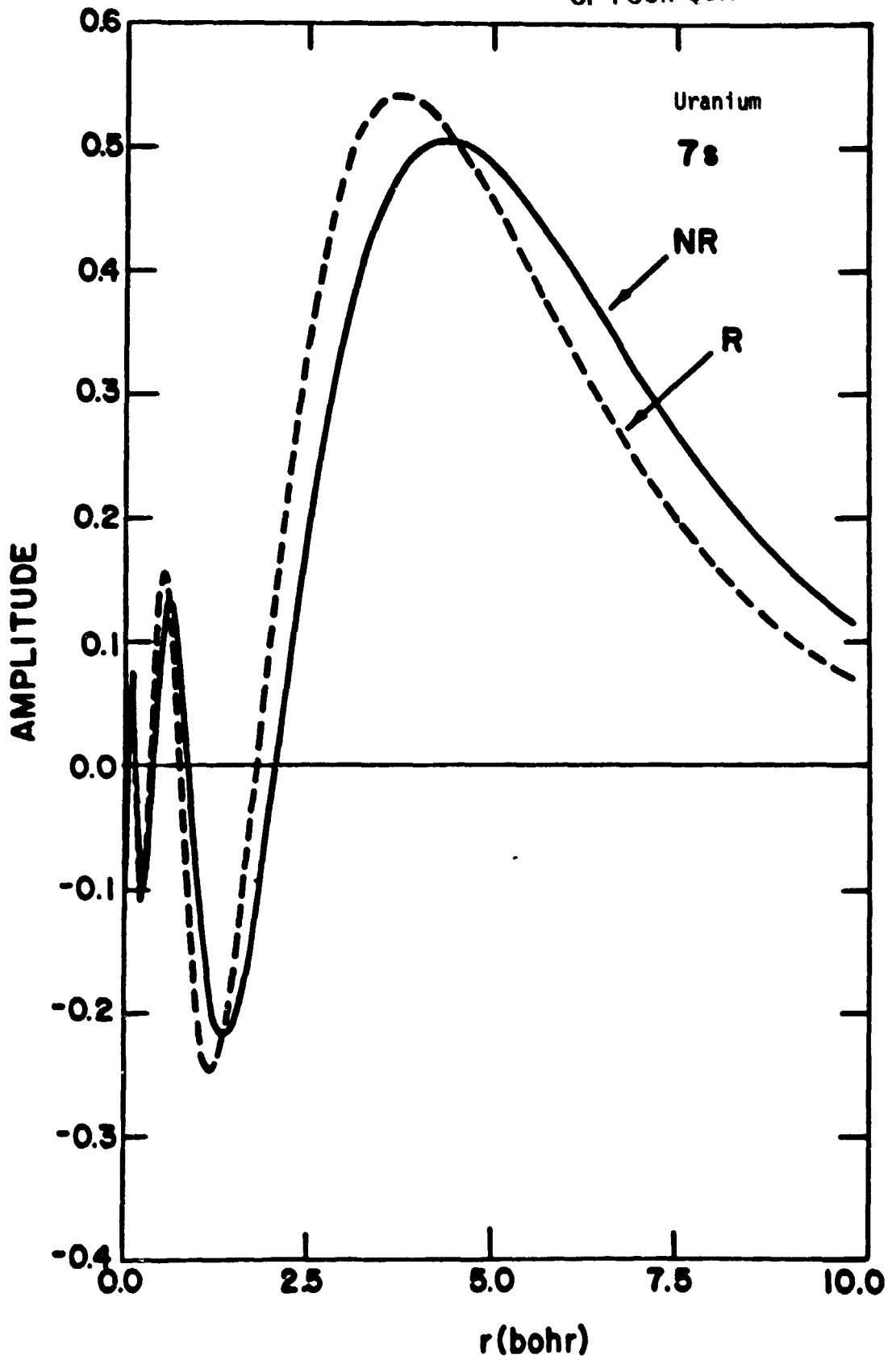

FIGURE 1. COMPARISON OF THE NON-RELATIVISTIC (NR) AND RELATIVISTIC (R) HARTREE-FOCK 7s ORBITALS IN URANIUM ATOM

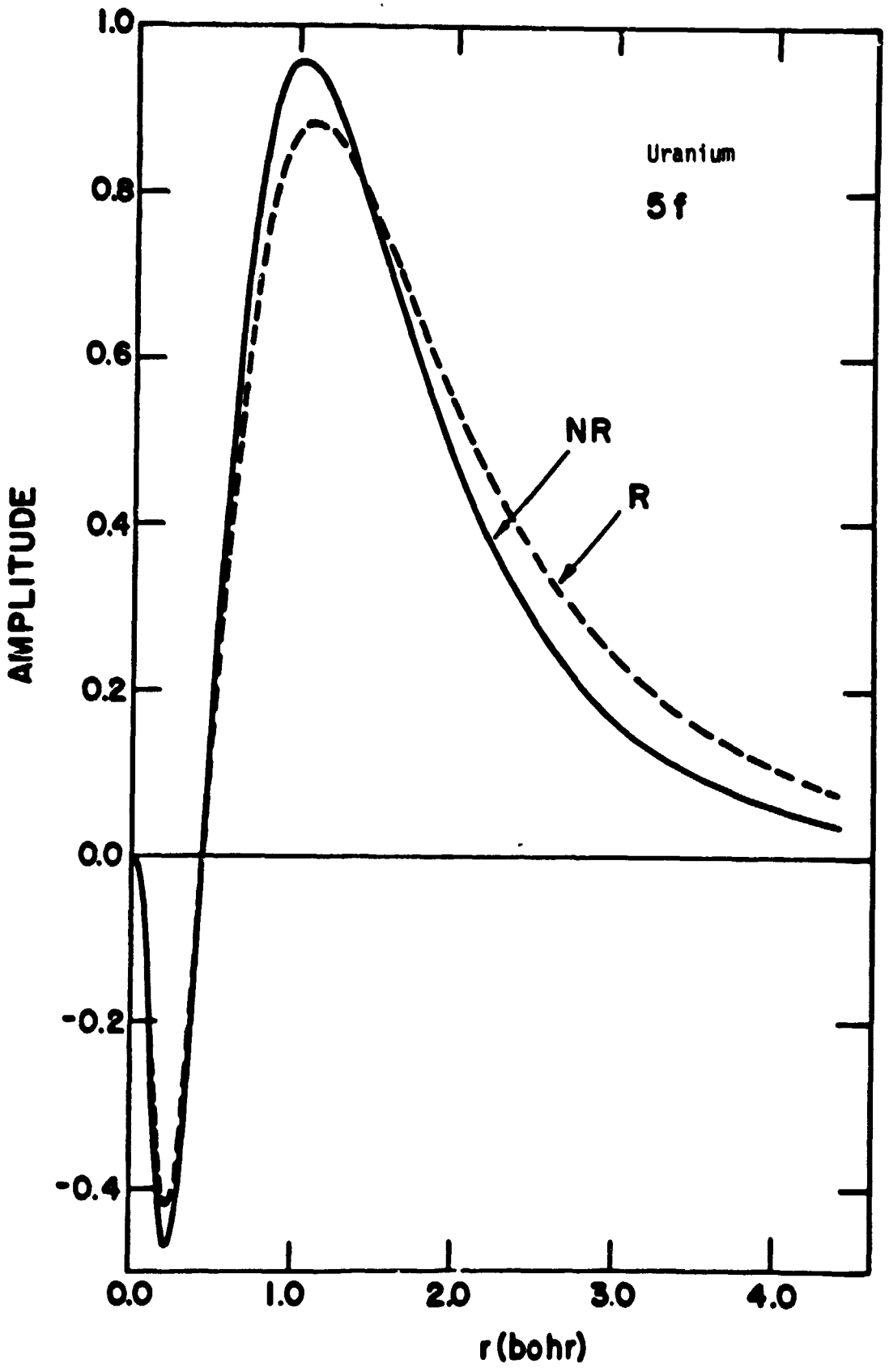

FIGURE 2. COMPARISON OF THE NON-RELATIVISTIC (NR) AND RELATIVISTIC (R) HARTREE-FOCK 5f ORBITALS IN URANIUM ATOM

Table 1. Comparison of Orbital Sizes and Energies for the Uranium Atom. (Ref. 6)

	RF[a]	RRF[b]	DHF[c]	DHF (average)
		$\langle r^2 \rangle$ (bohr^2)		
$5f_-$	1.94	2.57	2.53	2.61
$5f_+$			2.67	
$6d_-$	9.63	12.4	11.1	12.7
$6d_+$			13.7	
7s	28.8	21.5	21.8	21.8
$6p_-$	4.11	3.73	3.13	3.76
$6p_+$			4.08	
		Orbital Energy (a.u.)		
$5f_-$	-0.634	-0.331	-0.352	-0.320
$5f_+$			-0.297	
$6d_-$	-0.267	-0.188	-0.208	-0.186
$6d_+$			-0.172	
7s	-0.167	-0.201	-0.199	-0.199
$6p_-$	-1.04	-1.086	-1.363	-1.094
$6p_+$			-0.959	

[a] Nonrelativistic Hartree-Fock.
[b] Relativistic Hartree-Fock (Cowan-Griffin).
[c] Dirac-Hartree-Fock.

Table 2. Excitation Energies for the Au Atom. (Ref. 9)

	Excitation Energy (eV)			
	HF	RHF	DHF (avg)	Expt
$5d^{10}\ 6s^1(^2S)$	0.00	0.00	0.00	0.00
$5d^9\ 6s^2\ (^2D)$	5.13	1.86	1.86	1.74
$5d^{10}\ 6p^1\ (^2P)$	2.71	4.24	4.24	4.95

We review the basic properties of the RECP's next, and for this purpose confine the illustrative example to a nonrelativistic case. Consider for the sake of illustration an atom with a single valence electron such as the Li atom. The atomic equation for the valence orbital is written schematically as

$$\left(-\frac{1}{2}\frac{d^2}{dr^2} + \frac{\ell(\ell+1)}{2r^2} - \frac{Z}{r} + \hat{U} \right) P = \epsilon P \qquad (10)$$

where $\hat{U}$ physically represents all the interactions with all other electrons which, in this illustration, are the core electrons. This equation is assumed to have been solved. We define a local potential to simulate the effect of the nonlocal $\hat{U}$ by[10]

$$U^{LOCAL}(r) = \frac{\hat{U} P}{P} \qquad (11)$$

with the property that it ensures by construction that, given $\hat{U}$ and P, Equation (10) is simulated by

$$\left(-\frac{1}{2}\frac{d^2}{dr^2} + \frac{\ell(\ell+1)}{2r^2} - \frac{Z}{r} + U^{LOCAL}(r) \right) P = \epsilon P \qquad (12)$$

We show in Figure 3 a nodeless valence orbital (P/r) corresponding to the 2s orbital in Li atom.[10] This figure also shows another choice

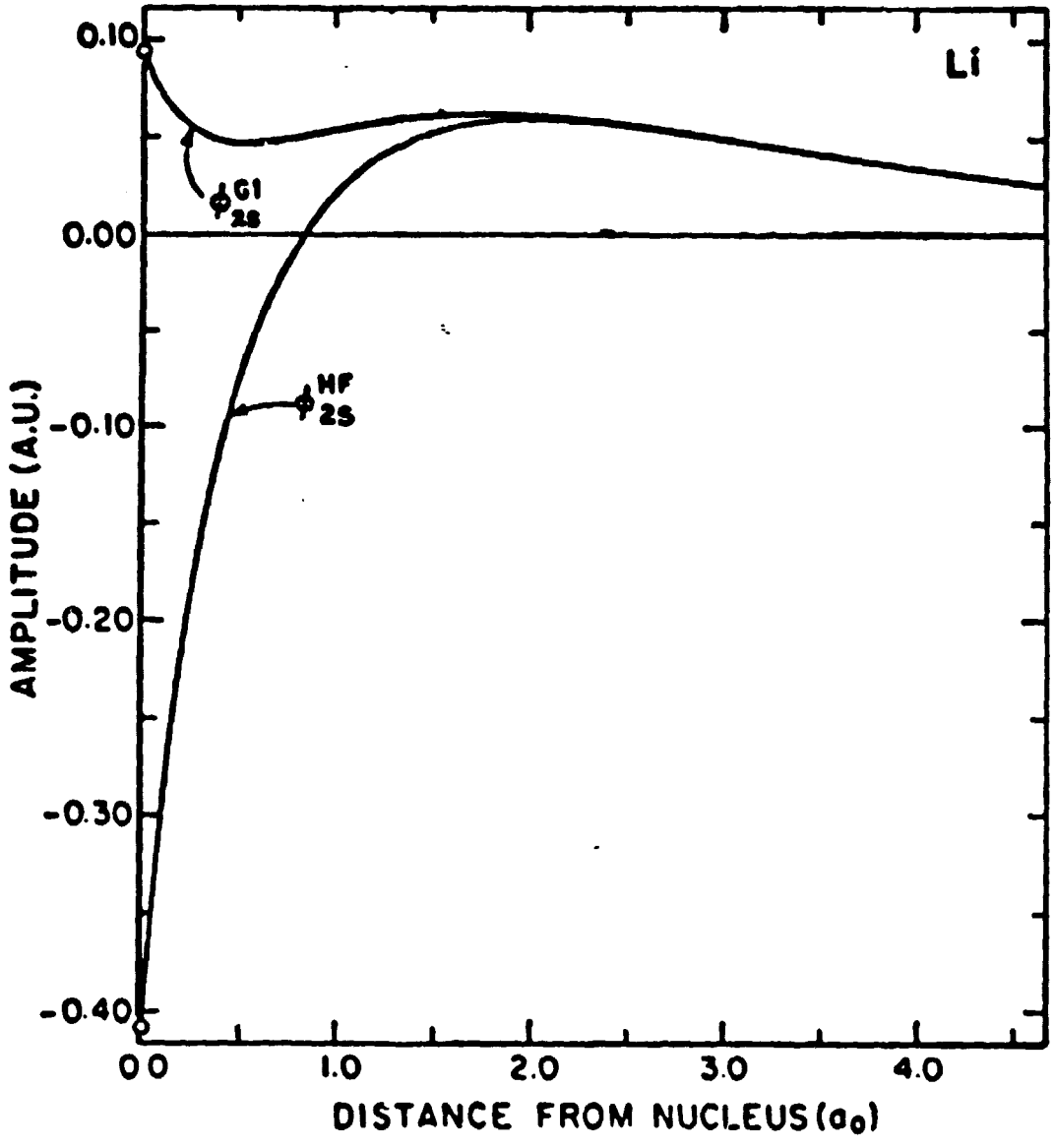

FIGURE 3. A NODELESS 2s ORBITAL IN LITHIUM ATOM, ϕ^{GI}_{2s}, AND THE CORRESPONDING NODEFUL 2s HARTREE-FOCK ORBITAL

for the 2s orbital which contains a node. We want to gloss over the important complications of the various other choices of P here and focus on the nodeless one in order to maintain the simplicitv of the discussion. Using the nodeless 2s orbital one obtains the potential shown labeled as U_s in Figure 4.[10] Indeed a different potential is obtained depending on whether the valence orbital is the 2p or 3d orbital, etc., and this yields the other potentials in Figure 4 labeled as U_p and U_d.[11] It is found that each such potential is the appropriate one for the spectrum of states of its own angular momentum as is schematically illustrated in Figure 5. This points out the important angular momentum dependence of the local potentials, and it explains the construction of the net ECP in terms of these local potentials combined with angular momentum projection operators as in[11]

$$U^{ECP} = \sum_{\ell=0}^{\infty} \sum_{m=\ell}^{-\ell} |\ell m\rangle U_\ell^{LOCAL}(r) \langle \ell m| \qquad (13)$$

The effects onto the valence electrons embodied in the ECP's are brought into the molecular calculations via the effective valence electron molecular hamiltonian,

$$H^{VAL.} = \sum_{\phi} \left[-\tfrac{1}{2}\nabla^2 + \sum_A \left(-\frac{Z_A}{r_A} + U_A^{ECP} \right) \right]_\phi + \sum_{\phi>\phi'} \sum \frac{1}{r_{\phi,\phi'}} \qquad (14)$$

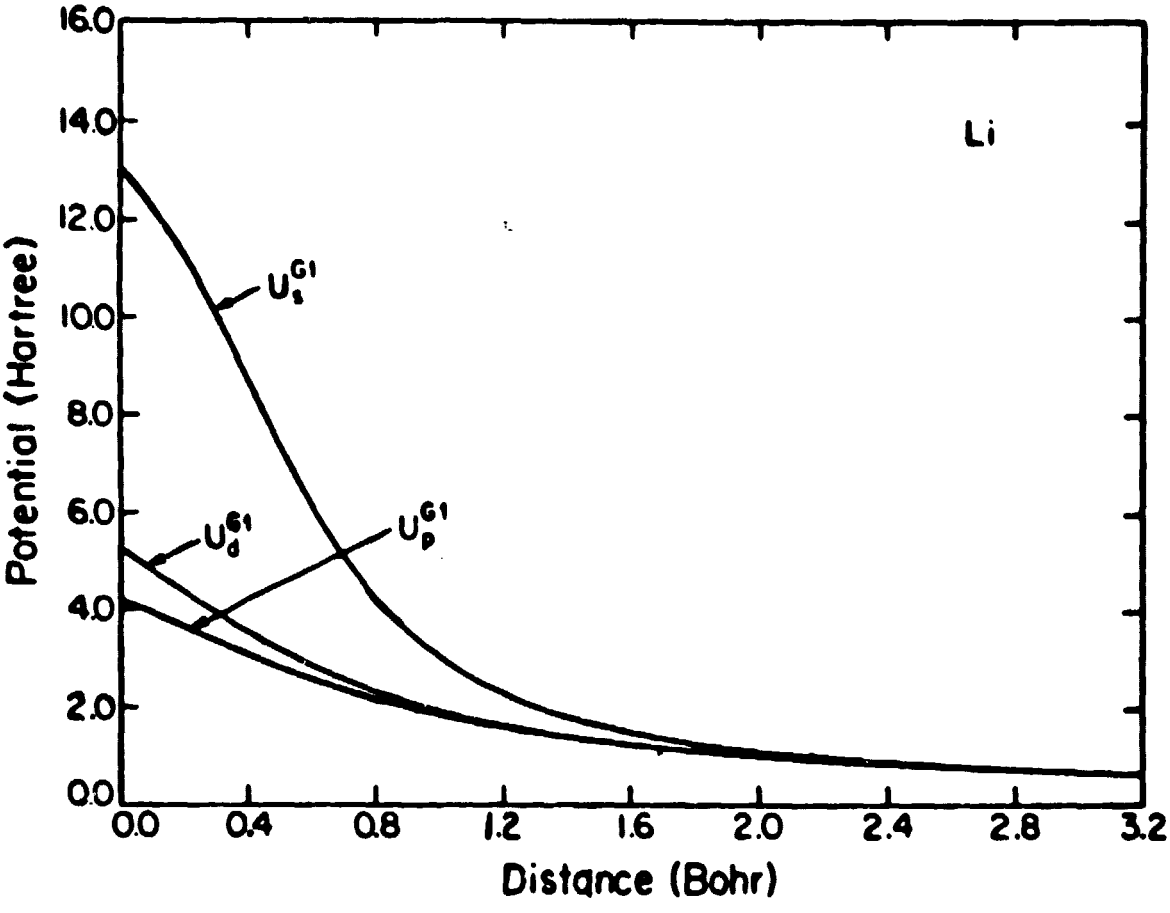

FIGURE 4. THE s, p, AND d LOCAL EFFECTIVE CORE POTENTIALS FOR THE LITHIUM ATOM

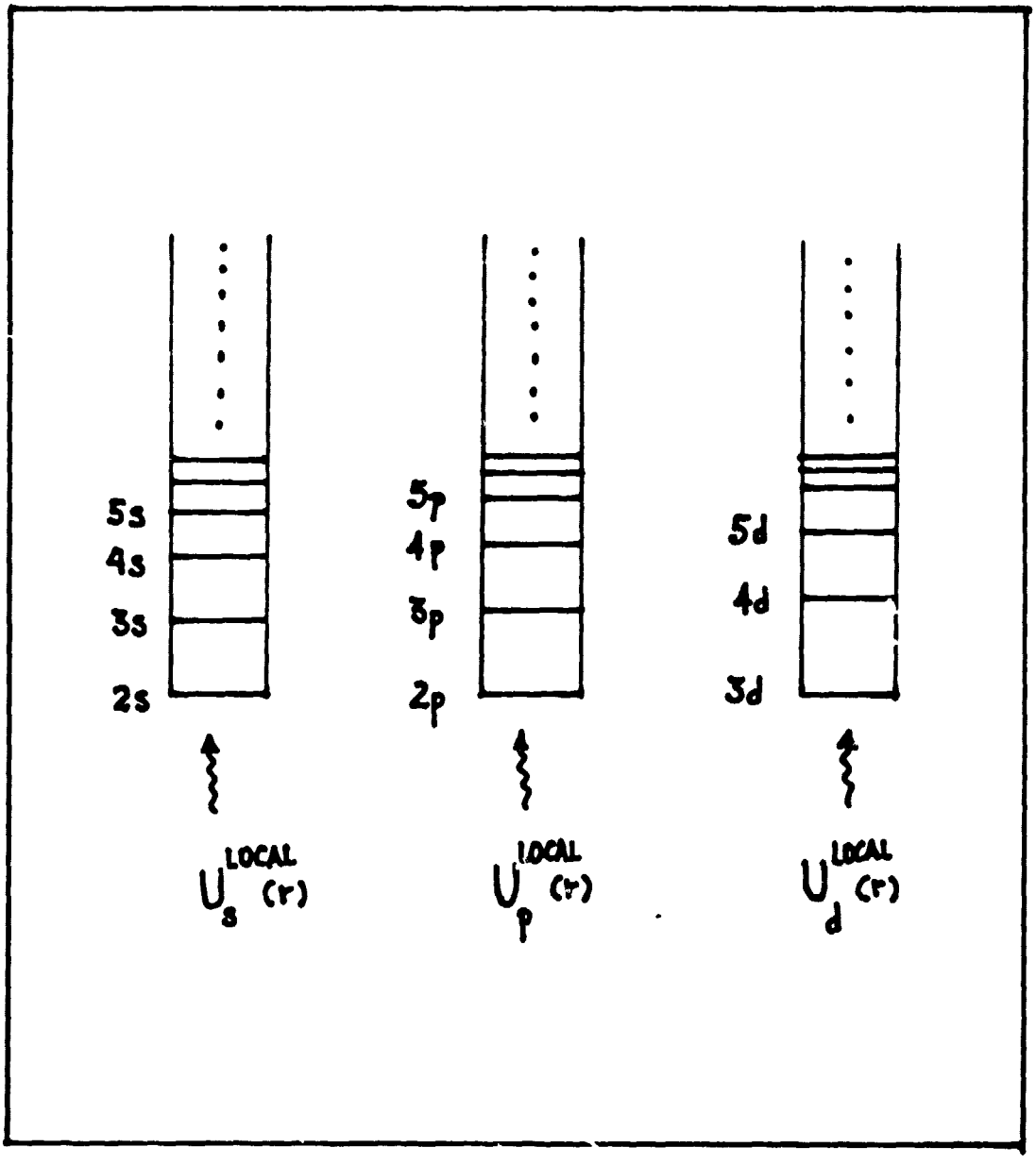

FIGURE 5. SCHEMATIC REPRESENTATION OF THE ONE-ELECTRON ORBITAL SPECTRUM ASSOCIATED WITH THE s, p, and d LOCAL EFFECTIVE CORE POTENTIALS FOR THE LITHIUM ATOM, RESPECTIVELY

Apart from the ECP, all other operators in Equation (14) are the usual non-relativistic operators, and they range only over the valence electrons. Thus, the only new element in carrying out a molecular calculation with ECP's is the evaluation of integrals of the ECP in a molecular basis. Computer programs to calculate these new integrals routinely are found integrated in various quantum chemistry packages. Whereas in special cases (e.g., diatomic molecules) it is efficient to evaluate the integrals using the ECP in its numerical form[11], for polyatomic calculations in a gaussian basis this direct approach has as yet been found prohibitively inefficient.[11] It is found, however, that if the ECP is first fit with analytical gaussian forms such as

$$\sum_i d_i \, r^{n_i} \exp\left[-\zeta_i r^2\right] \quad , \tag{15}$$

then the multicenter integrals can be efficiently calculated.[12] Therefore, polyatomic calculations with ECP's presently use the above noted expansions of the ECP's.[13]

A direct comparison of the valence molecular orbitals resulting from all-electron (AE) and valence-electron (VE) calculations for the molecules LiH $X^1\Sigma^+$ and Li_2^+ $X^2\Sigma_g^+$ was possible since the AE and VE orbitals could be calculated from directly comparable generalized Valence Bond wavefunctions[11]. This comparison is shown in Figures 6 and 7 for the LiH and Li_2^+ molecules, respectively. The comparison shows the AE and VE molecular orbitals to be virtually identical thereby establishing confidence in the validity of the basic ECP approach.[11]

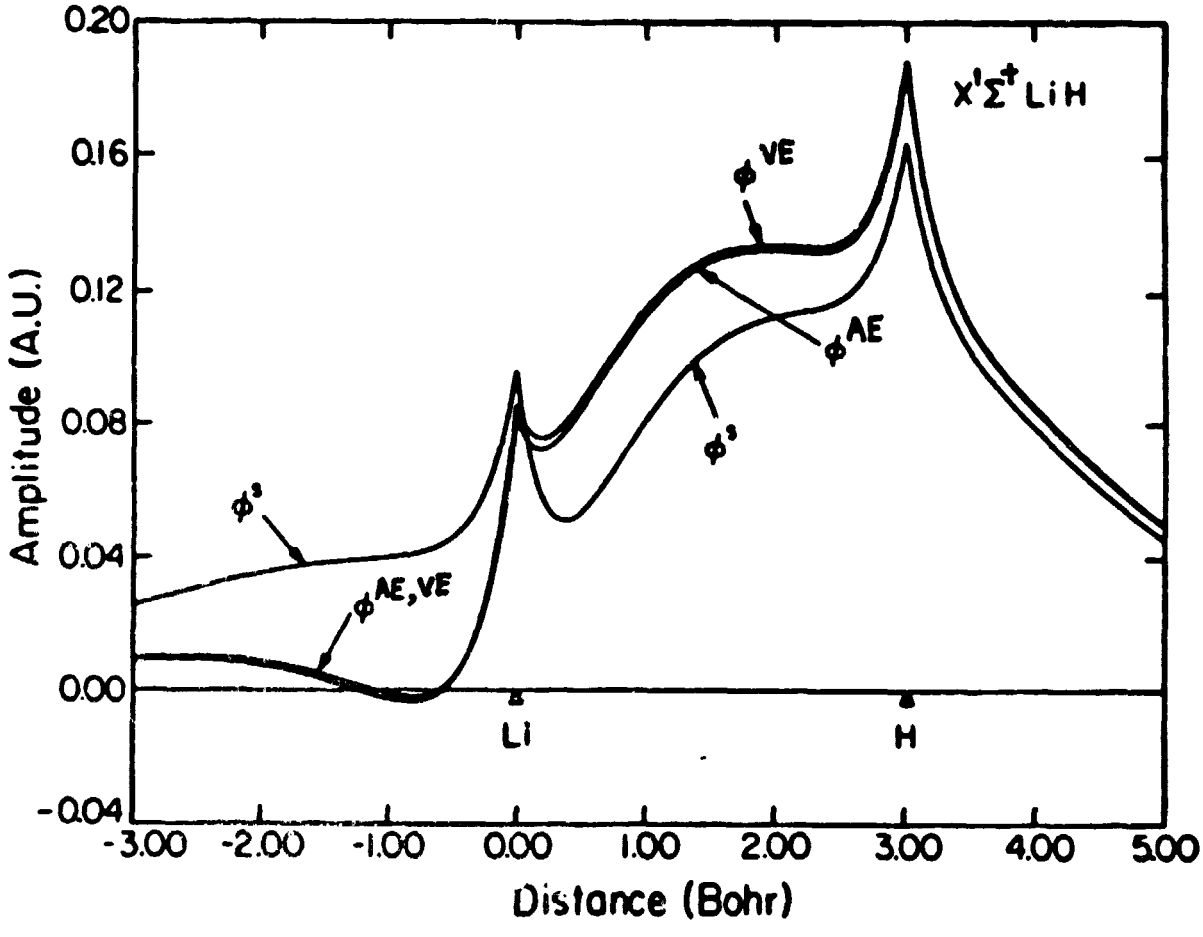

FIGURE 6. COMPARISON OF A VALENCE MOLECULAR ORBITAL FOR LiH $X'\Sigma^+$ OBTAINED FROM THE VALENCE ELECTRON (VE) ECP CALCUALTION AND A COMPARABLE ALL-ELECTRON (AE) CALCULATION

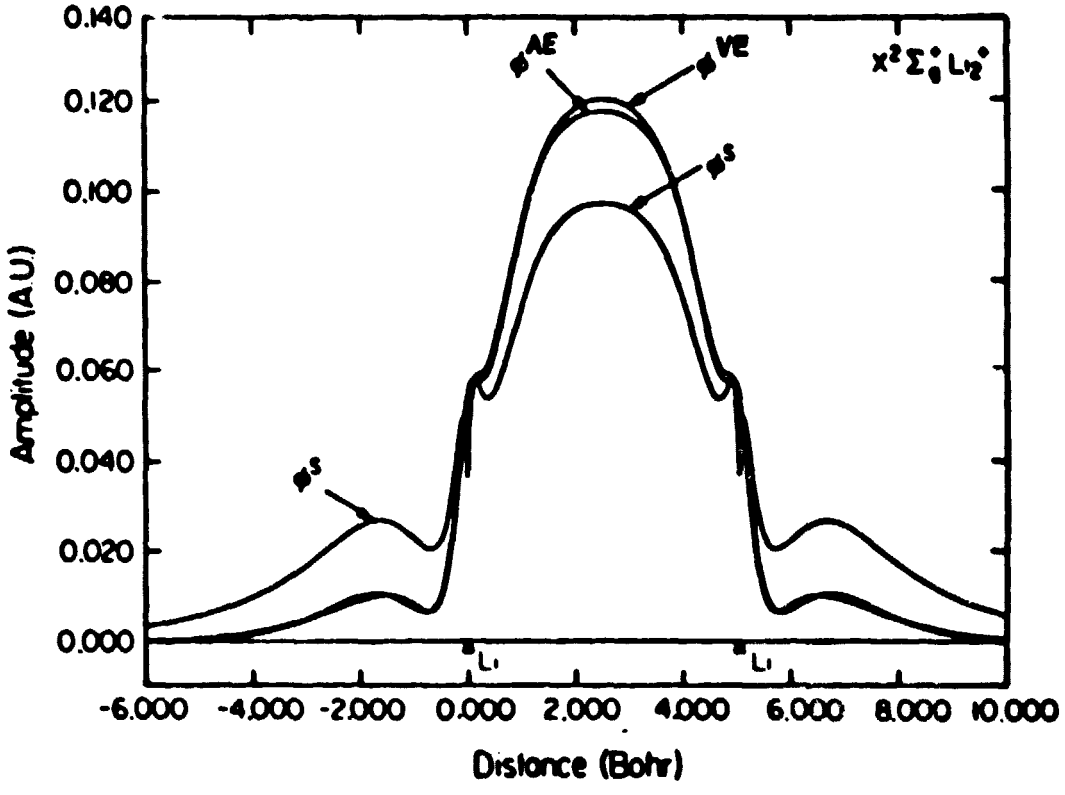

FIGURE 7. COMPARISON OF THE VALENCE MOLECULAR ORBITAL FOR Li_2^+ $X^2\Sigma^+$ OBTAINED FROM THE VALENCE ELECTRON (VE) ECP CALCULATION AND A COMPARABLE ALL-ELECTRON (AE) CALCULATION

The relativistic ECP's, or RECP's, are based on the one-component Cowan-Griffin (RHF) equation. The RHF equation for a valence orbital $P_{n\ell}$ is assumed to have been solved, and to have the form

$$\left[-\frac{1}{2}\frac{d^2}{dr^2} + \frac{\ell(\ell+1)}{2r^2} - \frac{Z}{r} + U^{CORE} + U^{REL.} + U^{VAL.}_{n\ell}\right]P_{n\ell} = \epsilon_{n\ell} P_{n\ell} \qquad (16)$$

where U^{CORE} consists of the interactions with the core electrons, U^{REL} consists of the relativistic mass-velocity and Darwin terms, and U^{VAL} consists of the interactions with the other valence electrons. To construct the RECP from this starting point, one seeks to obtain a new valence orbital (pseudo-orbital), $\tilde{P}_{n\ell}$, and a local potential, $U_\ell(r)$, that combine to satisfy the equation

$$\left[-\frac{1}{2}\frac{d^2}{dr^2} + \frac{\ell(\ell+1)}{2r^2} - \frac{Z}{r} + U_\ell(r) + \tilde{U}^{VAL.}_{n\ell}\right]\tilde{P}_{n\ell} = \epsilon_{n\ell}\tilde{P}_{n\ell} \qquad (17)$$

The local potential is defined as[7,14]

$$U_\ell(r) = \epsilon_{n\ell} - \frac{\left[-\frac{1}{2}\frac{d^2}{dr^2} + \frac{\ell(\ell+1)}{2r^2} - \frac{Z}{r} + \tilde{U}^{VAL.}_{n\ell}\right]\tilde{P}_{n\ell}}{\tilde{P}_{n\ell}} \qquad (18)$$

The $\tilde{U}^{VAL}$ term differs from the U^{VAL} term of Equation (16) in that, where appropriate, the valence interactions are constructed from the valence pseudo-orbitals, $\tilde{P}_{n\ell}$, rather than the original valence orbitals, $P_{n\ell}$.

The detailed properties of the valence pseudo-orbitals, $\tilde{P}_{n\ell}$, in Equation (18) are of critical importance in determining the reliability of the RECP's. The RECP itself may be thought of as a device for the embedding of the valence orbital properties. We shall discuss some of these orbital properties in greater detail in a subsequent section. Here we only point out three broad desired characteristics in constructing the valence pseudo-orbitals[12,13]:

(1) Nodelessness

(2) Maximum similarity with the parent valence orbital, $P_{n\ell}$

(3) Minimal special characteristics in the core region.

A schematic comparison of the parent valence orbital, $P_{n\ell}$, with two possible choices for the valence pseudo-orbitals, $\tilde{P}_{n\ell}$, is shown in Figure 8.

3. SPIN-ORBIT COUPLING

The one-component approach to molecular relativistic electronic structure calculations reviewed here does not include the effects of the spin-orbit coupling operator. The important effects of spin-orbit coupling have to be obtained in a subsequent calculation in which the energies E_I and states Ψ_I obtained from the RECP calculations are used to set up a net hamiltonian matrix

$$H_{I,J} = \delta_{I,J} E_I + \langle \Psi_I | \hat{V}_{SO} | \Psi_J \rangle \qquad (19)$$

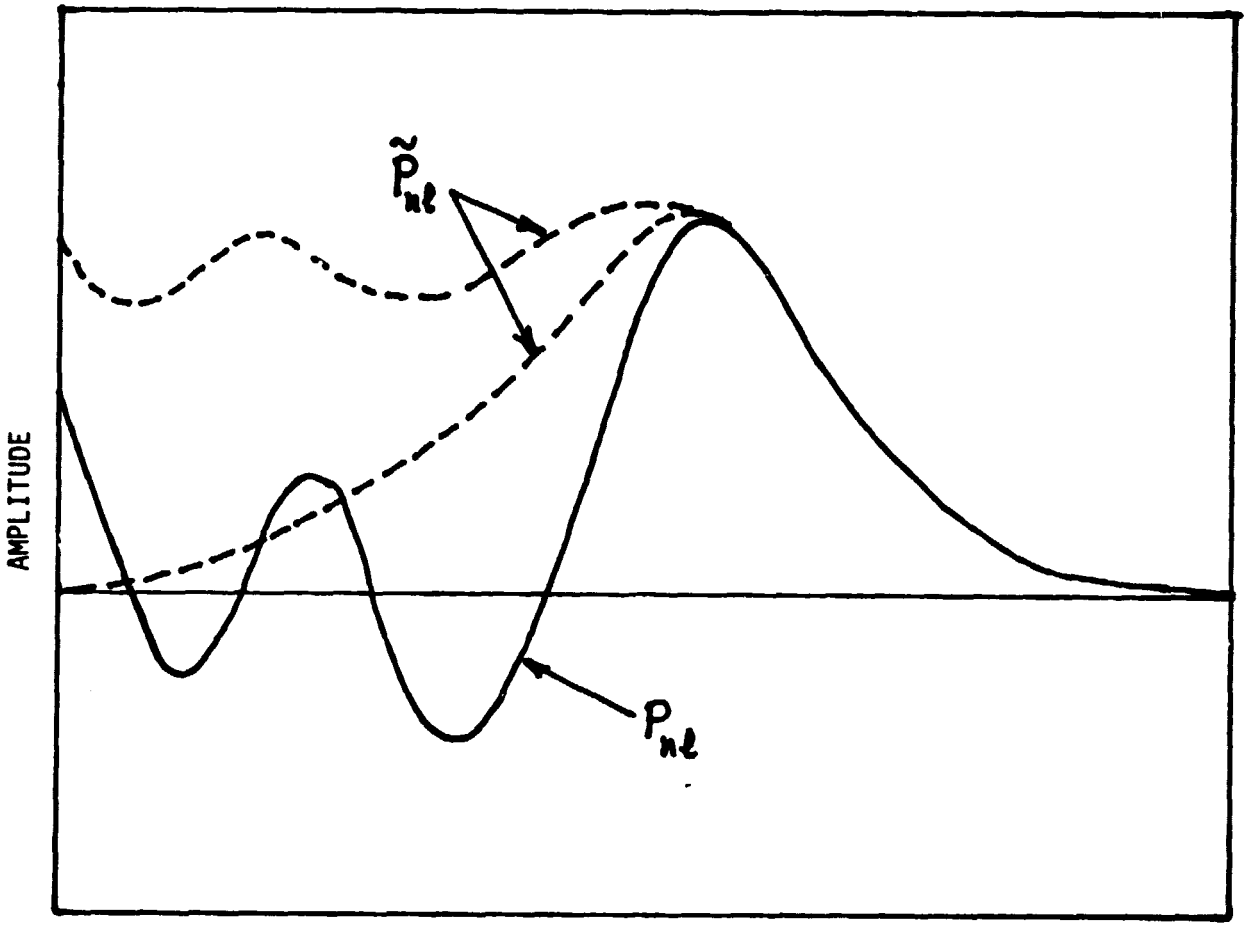

FIGURE 8. SCHEMATIC COMPARISON OF TWO POSSIBLE VALENCE PSEUDO-ORBITALS, $\tilde{P}_{N\ell}$, WITH THE PARENT HARTREE-FOCK VALENCE ORBITAL, $P_{n\ell}$

The hamiltonian matrix is then diagonalized to obtain the molecular energy in the presence of the spin-orbit operator, $\hat{V}_{SO}$.

Three levels of decreasing sophistication but also of decreasing computational difficulty have emerged in recent years for the calculation of the spin-orbit matrix elements, $\langle \Psi_I | \hat{V}_{SO} | \Psi_j \rangle$ These are:

(1) Use of the rigorous spin-orbit interaction of the Breit-Pauli hamiltonian requiring the computation of one-electron and two-electron multi-center integrals

(2) Use of an effective one-electron operator of the form

$$\hat{V}_{SO} = \sum_i \sum_A \xi_A(r_{i,A}) \vec{\ell}_{i,A} \cdot \vec{s}_i \qquad (20)$$

where is sum is over the nuclear centers, A.

(3) Use of the "atoms-in-molecules" method.

3.1. Atoms-In-Molecules

The computationally simplest and quickest approach to obtain some semiquantitative measure of the effect of spin-orbit coupling on the molecular states calculated using the RECP's is the atoms-in-molecules approach.[15] The approximation is valid when the molecular states retain the same spin-orbit coupling as the parent atomic states. The spin-orbit matrix element $\langle \Psi_I | \hat{V}_{SO} | \Psi_J \rangle$ are assumed to depend on the spin-orbit splittings of the constituent fragments, and remain constant as the atoms are brought together to form the molecule.

To illustrate this approach we consider the XeF molecule.[16] The potential energy curves calculated with an RECP but prior to including spin-orbit coupling are shown in Figure 9. The atomic ionic limit splits upon introducing spin-orbit coupling

$$Xe^+(^2P) + F^-(^1S) \begin{cases} \rightarrow Xe^+(^2P_{1/2}) + F^-(^1S_0) \\ \rightarrow Xe^+(^2P_{3/2}) + F^-(^1S_0) \end{cases} \qquad (21)$$

Let λ be half of the spin-orbit splitting between the $Xe^+(^2P_{1/2})$ and $Xe^+(^2P_{3/2})$ states. The atoms-in-molecules approximation yields the net hamiltonian matrix.[17]

$$\begin{pmatrix} E_{2^2\Sigma^+}(R) & -\lambda\sqrt{2} & 0 \\ -\lambda\sqrt{2} & E_{2^2\Pi}(R) + \lambda & 0 \\ 0 & 0 & E_{2^2\Sigma^+}(R) - \lambda \end{pmatrix} \qquad (22)$$

The molecular states obtained by diagonalizing this matrix are shown in Figure 10. In turn, the emission wavelengths to the ground states calculated from these curves are given in Table 3.[16] This table shows that the correspondence between the calculated and the experimentally observed emission wavelengths is unambiguous. The ready assignment of the emission wavelengths that follows in this example shows the usefulness of

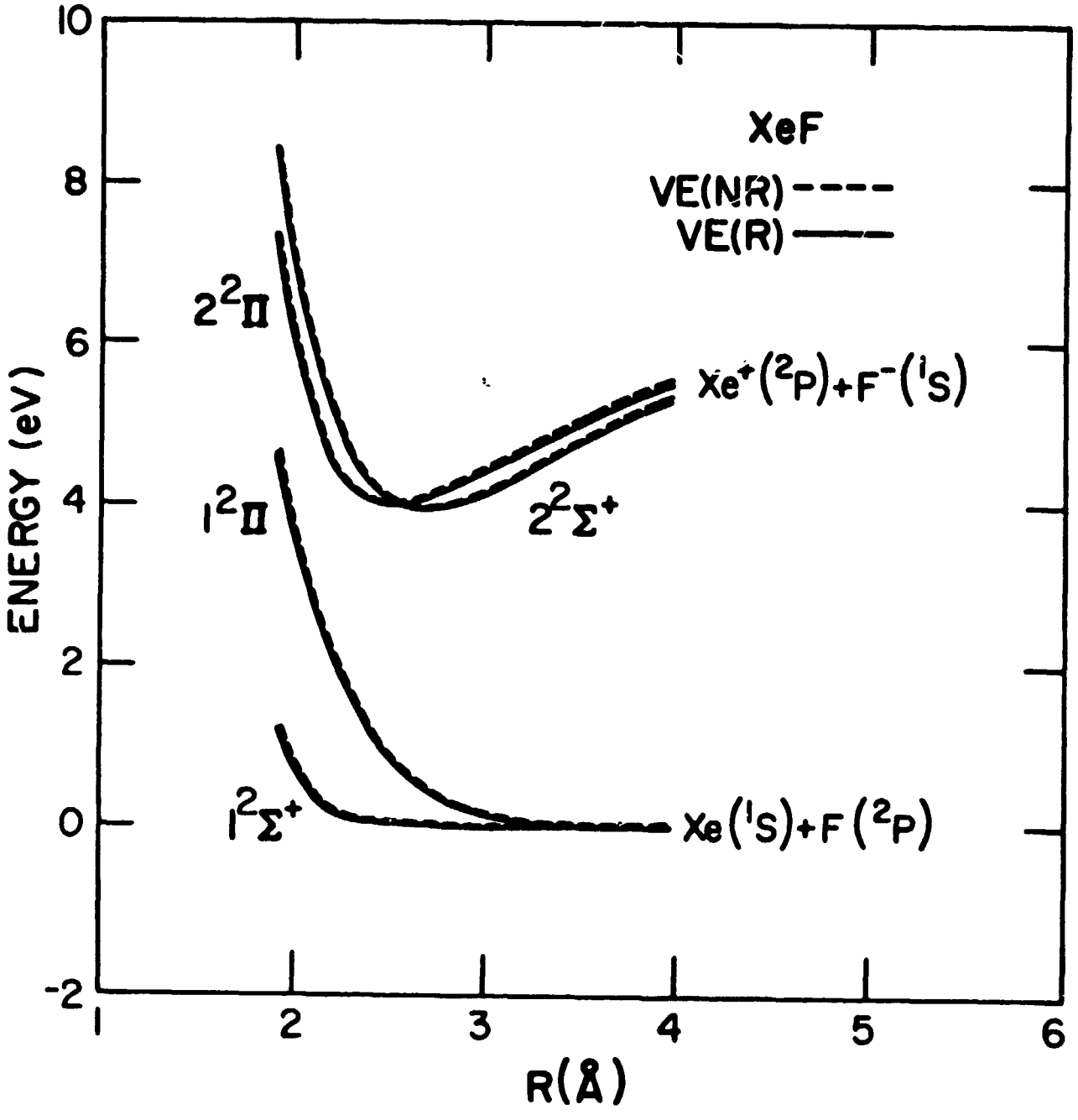

FIGURE 9. COMPARISON OF THE NONRELATIVISTIC (NR) AND RELATIVISTIC (R) VALENCE ELECTRON (VE) POTENTIAL ENERGY CURVES FOR THE LOW-LYING ELECTRONIC STATES OF THE XeF MOLECULE PRIOR TO THE INCLUSION OF THE SPIN-ORBIT EFFECTS

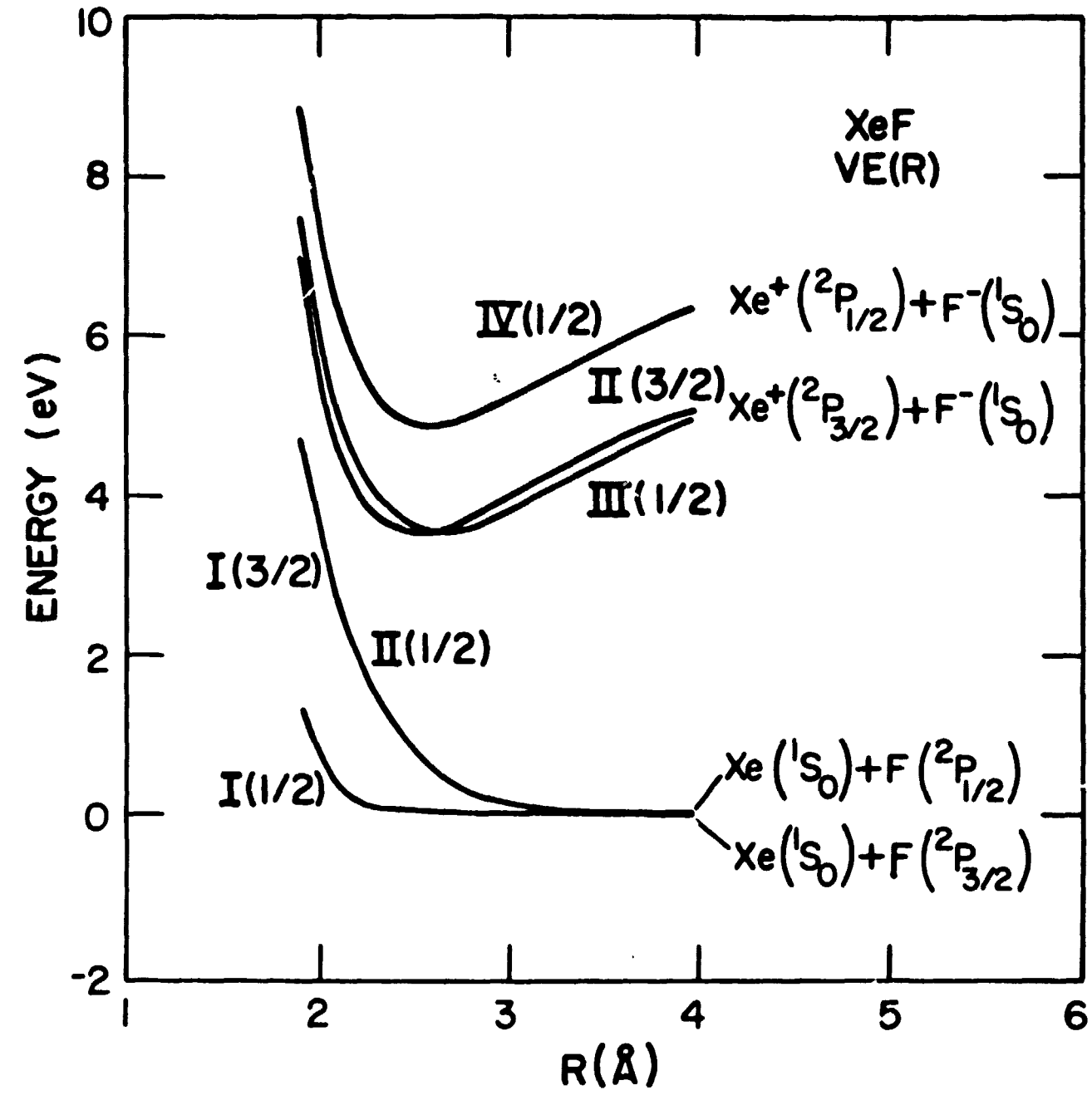

FIGURE 10. THE RELATIVISTIC (R) VALENCE ELECTRON (VE) POTENTIAL ENERGY CURVES FOR THE LOW-LYING ELECTRONIC STATES OF THE XeF MOLECULE INCLUDING SPIN-ORBIT EFFECTS (USING THE ATOMS-IN-MOLECULES APPROXIMATION)

Table 3. Emission Wavelengths (nanometer) in XeF Molecule.[a]

TRANSITION	CALCULATED	EXPERIMENT
$III_{1/2} \rightarrow I_{1/2}$	340	352
$IV_{1/2} \rightarrow I_{1/2}$	249	264
$II_{3/2} \rightarrow I_{3/2}$	422	450
$2^2\Sigma^+ \rightarrow 1^2\Sigma^+$	307	
$2^2\Pi \rightarrow 1^2\Pi$	368	

[a] W.R. WADT, P.J. HAY, L.R. KAHN, J. CHEM. PHYS. 68, 1752 (1978)

this simple approximation in giving a quick broad guide to the effects of spin-orbit coupling. Note that the emission wavelengths prior to including the atoms-in-molecules spin-orbit effects, also given in Table 3, provide no correlation with the experimental emission wavelengths.

3.2. Effective One-Electron Spin-Orbit Operators

The most rigorous approach to the inclusion of spin-orbit effects is the use of the full molecular spin-orbit term in the Breit-Pauli hamiltonian[18],

$$\hat{V}_{SO} = \frac{\alpha^2}{2}\left\{ \sum_i \sum_A \frac{Z_A}{r_{A,i}^3} \left| \vec{r}_{A,i} \times \vec{p}_i \right| \cdot \vec{s}_i + \sum_{i \neq j} \sum \left| \frac{\vec{r}_{ij}}{r_{ij}^3} \times \vec{p}_i \right| \cdot \left| \vec{s}_i + 2\vec{s}_j \right| \right\} \qquad (23)$$

This is also the computationally most difficult approach since it requires the computation of multicenter integrals of both one-electron and two-electron integrals. Although such molecular computations are now feasible[19-22], they remain the exception rather than the norm because of the associated computational difficulty. There is therefore a need to find reliable approximations to Equation (23) that go beyond the atoms-in-molecules approach in dealing with the changes that occur as the atoms are brought together, and that yet remain computationally practical.

The increasingly large numbers of chemically inert core electrons as one moves down the periodic table are an even larger computational obstacle to the use of the rigorous molecular spin-orbit interaction, Equation (23),

than they are for the calculation of the nonrelativistic molecular energy. The problem lies in the presence of the two-electron spin-orbit operators. There is, however, good reason to think that the dominant contribution of these two-electron spin-orbit operators is contained in the interaction between core and valence electrons mediated by this operator. Indeed, examination of values of all integrals needed for the evaluation of the matrix element $\langle {}^3\Sigma_g^- | \Omega_{SO} | {}^1\Sigma_g^+ \rangle$ for the oxygen molecule, for example, shows the core-valence two-electron spin-orbit integrals to be <u>one order of magnitude</u> larger than the valence-valence two-electron spin-orbit integrals.[21]

It is possible to isolate the specific form of the two-electron core-valence spin-orbit interaction. We take as example the manner in which the analogous problem has been solved in the nonrelativistic case.[23] It is well known that the two-electron core-valence nonrelativistic interactions can be expressed as a net potential due to the core electrons,

$$\sum_c \left(2\hat{J}_c - \hat{K}_c \right) \quad . \tag{24}$$

acting on the valence electrons (the sum in Equation (24)) is over all core orbitals). This potential is combined with remaining valence operators to yield the nonrelativistic effective valence-electron hamiltonian,

$$H^{VAL} = \sum_v \left[-\tfrac{1}{2}\nabla^2 - \sum_A \frac{Z_A}{r_A} + \sum_c \left(2\hat{J}_c - \hat{K}_c \right) \right]_v + \sum_{v>v'} \sum \frac{1}{r_{v,v'}} \tag{25}$$

where the operator indexes range only over the valence electrons.[23]

Applying the same approach to the rigorous spin-orbit interaction, Equation (23), we start by partitioning the many-electron wavefunction. We divide the all-electron one-component wavefunction into a Cowan-Griffin set of core orbitals, $\{\phi_c\}$, and an unspecified valence wavefunction orthogonal to these core-orbitals, Θ^{VAL},

$$\Psi = \mathcal{A}\left| \phi_1^2 \phi_2^2 \cdots \phi_n^2 \; \Theta^{VAL.} \right| \tag{26}$$

where $\mathcal{A}$ stands for the antisymmetrizer. Integrating the rigorous spin-orbit interaction, $\hat{V}_{SO}$, over the core-electrons and combining the resulting core-valence terms with the valence-valence terms, we find the following effective valence-electron spin-orbit interaction:[24]

$$\hat{V}_{SO}^{VAL.} = \frac{\alpha^2}{2}\left\{ \sum_v \left[\nabla\left(-\sum_A \frac{Z_A}{r_A} + \sum_c \left| 2\hat{J}_c + 2\hat{K}_c \right|\right) \times \hat{p} \right]_v \cdot \hat{\Delta}_v \right.$$

$$\left. + \sum_{v \neq v'} \sum \left(\frac{\vec{r}_{v,v'}}{r^3_{v,v'}} \times \hat{p}_v \right) \cdot \left(\vec{\Delta}_v + 2\vec{\Delta}_{v'} \right) \right\} \tag{27}$$

where the operator indexes range only over the valence electrons. The remaining core-core terms are all zero.

The core electrons are shown by Equation (27) to formally contribute to the effective valence-electron spin-orbit interaction via the gradient of the potential

$$\sum_{c} \left[2\hat{j}_c + 2\hat{K}_c \right] \tag{28}$$

Since this potential is of opposite sign to the nuclear potential, the core electrons can be said to "shield" the nucleus in the spin-orbit interaction analogously as in the nonrelativistic energy. On the basis of the localized atomic nature of the core orbitals, the potential in Equation (28) may be expressed as a superposition of atomic potentials each centered on one of the nuclei. Combining these atomic potentials with the nuclear potentials to obtain a net potential on each nucleus, v^{eff}, one may reexpress Equation (27) as

$$\hat{V}_{SO}^{VAL.} = \frac{\alpha^2}{2} \left\{ \sum_{\nu} \sum_{A} \left[\nabla v_A^{eff} \times \vec{p} \right]_{\nu} \cdot \vec{A}_{\nu} + \sum_{\nu \neq \nu'} \sum \left[\frac{\vec{r}_{\nu,\nu'}}{r^3_{\nu,\nu'}} \times \vec{p}_{\nu} \right] \cdot \left[\vec{A}_{\nu} + 2\vec{A}_{\nu'} \right] \right\} \tag{29}$$

where again the operator indexes range only over the valence electrons.

The bare nuclei one-electron spin-orbit terms are found in practice to be <u>two orders of magnitude</u> larger than the valence-valence two-electron spin-orbit interactions. The effective one-electron spin-orbit terms in

V_{SO}^{VAL}, Equation (29) in turn contain the "shielded" bare nuclei terms. These one-electron terms are expected to be thus at least an order of magnitude larger than the two-electron spin-orbit interaction remaining in Equation (29). On this basis, it is reasonable to expect approximate one-electron spin-orbit operators to account already for most of the chemically important molecular properties.

Whereas one-electron operators of some sophistication have been described recently in the literature,[25,26] we wish to illustrate here how well even simpler one-electron approximation appear to work.[17] This simplest of approximations is based on letting

$$v^{eff.} \simeq -\frac{Z^{eff}}{r} \tag{30}$$

to obtain the following approximation to Equation (29),

$$\hat{V}_{SO}^{VAL} \simeq \frac{\alpha^2}{2} \sum_{\nu} \sum_{A} \frac{Z_A^{eff}}{r_{A,\nu}^3} \vec{\ell}_{A,\nu} \cdot \vec{s}_{\nu} \tag{31}$$

Z^{eff} is a parameter adjusted to match either theoretical or experimental atomic spin-orbit parameters. Moreover, in molecular calculations all but the one-center integrals of Equation (31) are neglected. The latter condition can probably be removed by allowing the parameter Z^{eff} to have a radial dependence reflecting the increased shielding at larger distances from the nucleus. Table 4 shows spin-orbit parameters calculated for states

Table 4. Comparison of Silicon atom spin-orbit constants (in cm^{-1}) calculated by Stevens and Krauss (SK) (ref. 26) and by the effective one-electron one-center spin-orbit operator. (ref. 27)

State	VE (5s7p)	SK	SK(3+)[a]	Expt
Si $[3s^2 3p^2]$ ^3P	148.9	157.8	152.7	148.9
$Si^+[3s^2 3p^1]$ ^2P	179.9	201.4	196.3	191.3
$Si^+[3s^2 4p^1]$ ^2P	32.7	36.9	36.6	40.0
$Si^{3+}[3p^1]$ ^2P	250.2	--	310.1	306.9

[a] Same as SK except that the spin-orbit operator is derived from Si(3+) with the $(1s^2 2s^2 2p^6)$ core orbitals frozen as in Si (^3P).

of silicon atom wherein the valence 3p orbitals undergoes large changes. A reasonable comparison is still shown in Table 4 with the more sophisticated one-electron approximation as well as with experiment for all states (except Si^{3+}), notwithstanding the extreme simplicity of this effective one-electron approximation. Surprisingly good agreement with spin-orbit coupling matrix elements using the full Breit-Pauli hamiltonian between electronic states of the rare gas oxides ArO, KrO, and XeO as a function of internuclear distance is obtained by Langhoff[22] and shown in Figure 11.

4. REPRESENTATIVE APPLICATIONS

We briefly review next some representative molecular applications of the one-component approach to relativistic structure calculations discussed here.

To illustrate the relativistic effect on chemical bonds, we compare relativistic (R) and nonrelativistic (NR) calculations of the potential energy curves of the AuH and AuCl in their $X'\Sigma^+$ ground states.[9] The potential energy curves are compared in Figure 12 and Tables 5 and 6. It is observed that the equilibrium bond length is predicted to be smaller by the relativistic calculations in both cases. In AuH, for example, a bond contraction of 0.3 Å is predicted that yields a bond length differing by only 0.01 Å from the experimental value of 1.52 Å.

Since it has been traditional to correlate binding characteristics directly with orbital properties, we have interpreted[9] this bond contraction as originating in the relativistic contraction of the Au 6s bonding

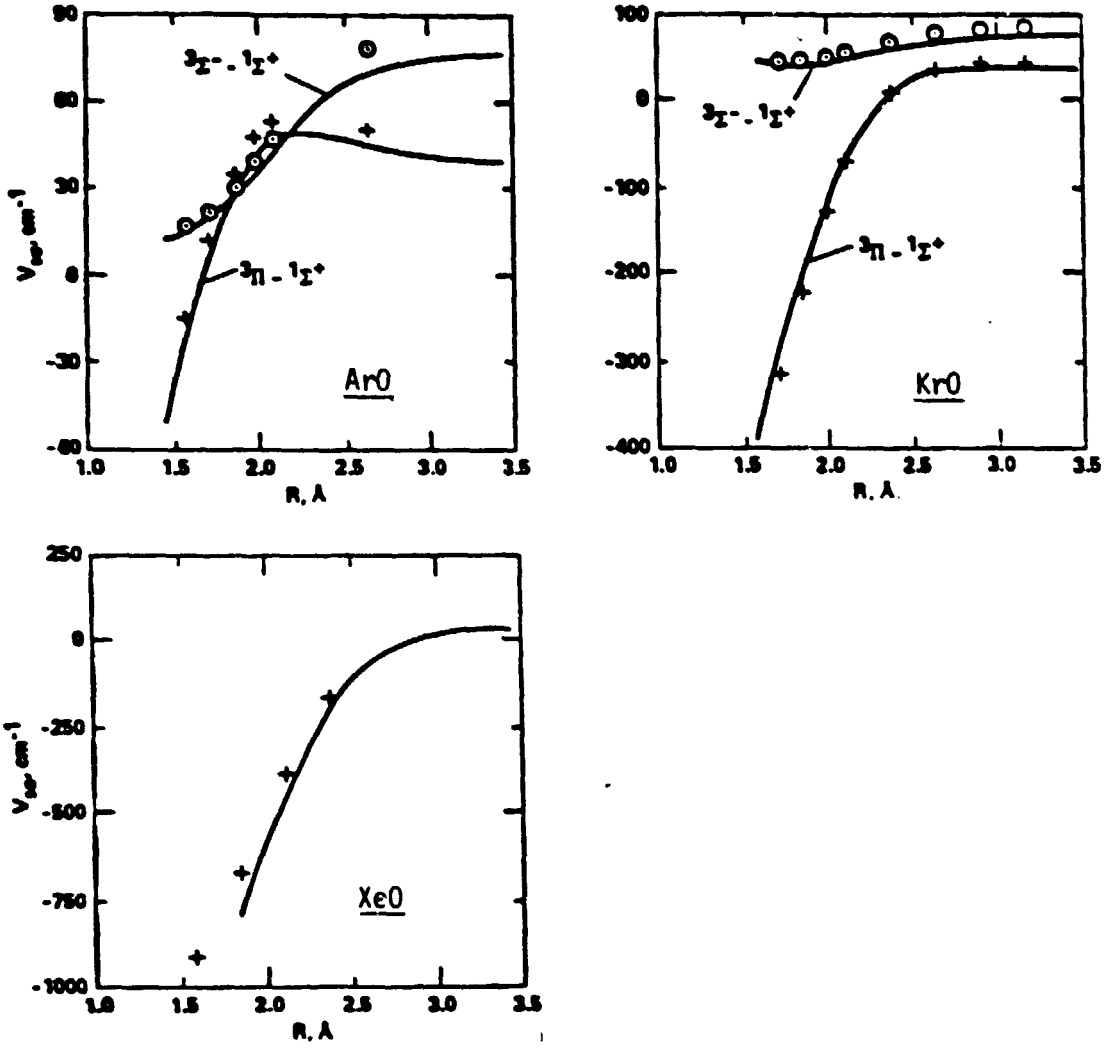

FIGURE 11. SPIN-ORBIT COUPLING MATRIX ELEMENTS BETWEEN ELECTRONIC STATES OF THE RARE GAS OXIDES COMPUTED BY LANGHOFF (REFERENCE 22) USING THE FULL BREIT-PAULI HAMILTONIAN (SOLID LINES) AND THE 1-ELECTRON 1-CENTER EFFECTIVE SPIN-ORBIT OPERATOR (CIRCLES AND CROSSES)

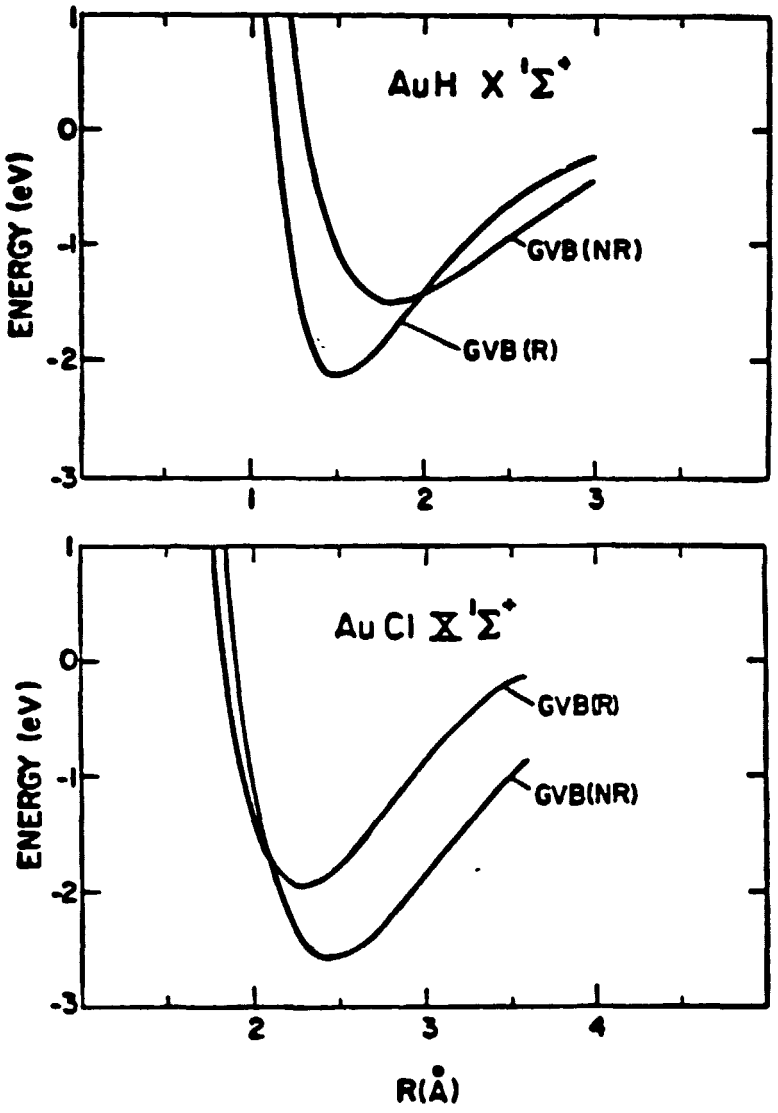

FIGURE 12. THE POTENTIAL ENERGY CURVES FOR THE GROUND STATES OF AuH AND AuCl OBTAINED USING A NONRELATIVISTIC (NR) AND RELATIVISTIC (R) ECP AND A GENERALIZED VALENCE BOND WAVEFUNCTION

Table 5. Spectroscopic Properties of AuH molecule[a]

AuH $(X^1\Sigma^+)$	R_e(Å)	D_e(eV)	ω_e(cm^{-1})
Nonrel. ECP			
HF	1.763	0.99	1387
GVB-1	1.820	1.52	1203
POL-CI	1.807	1.57	12.17
Rel ECP			
HF	1.508	1.55	2014
GVB-1	1.514	2.14	1891
POL-CI	1.522	2.23	1871
Exptl	1.5237	3.37	2305
1-Center Dirac-Fock			
Nonrel.	1.745	—	2296
Rel.	1.659	—	2178

[a]P. J. Hay, W. R. Wadt, L. R. Kahn, F. W. Bobrowicz, J. Chem. Phys., 64, 984 (1978).

Table 6. Spectroscopic Properties of AuCl Molecule[a]

AuCl ($X^1\Sigma^+$)	R_e(Å)	D_e(eV)	ω_e(cm^{-1})
Nonrel. ECP			
GVB-1	2.447	2.58	277
Rel. ECP			
GVB-1	2.283	1.96	298
POL-CI	2.291	2.39	306
Exptl	—	3.5 ± 0.1	382

[a] P. J. Hay, W. R. Wadt, L. R. Kahn, F. W. Bobrowicz, J. Chem. Phys., 69, 984 (1978)

orbital ($\langle r \rangle_{6s}$ is reduced from 3.7 Bohr to 3.0 Bohr). Ziegler, Snijders and Baerends[28], however, have established that the bond contraction first has its origin in the relativistic mass velocity and Darwin terms prior to their effect on the Au 6d orbital. It is indeed reasonable, in retrospect, that the same relativistic terms that would further attract the Au 6s orbital to the Au nucleus, and cause its relativistic contraction, should also attract the approaching hydrogen 1s orbital, the other bonding orbital, and thereby lead to the bond contraction.

The decrease in the binding energy in AuCl, an ionic molecule, is interpreted to be a result of the deferral to smaller internuclear distances of the onset of the admixture of the ionic configuration Au^+Cl^-.[9] The delay of this onset is the result of the increased energy of the $Au^+ + Cl^-$ asymptote relative to the covalent neutral atoms asymptote; it is caused by the relativistic energy stabilization of the Au 6s orbital.

Some of the important and exciting research problems for the application of relativistic molecular methods lie in the chemistry of transition-metal complexes.[29] We illustrate the applicability of the present one-component approach to these types of molecules with some results by Hay[30] on the $PtCl_3(C_2H_4)^-$ complex (Zeise's salt). Figure 13 shows good agreement in a comparison of the calculated geometric parameters of Zeise's salt computed using a Pt RECP, and the geometric parameters obtained from neutron diffraction experiments. Moreover, the perpendicular orientation of the ethylene ligand relative to the $PtCl_3^-$ plane is correctly predicted to be the stable form with the coplanar configuration lying 15 kcal/mol higher in energy. Finally, the bending of the CH_2 groups away from the Pt atom is also predicted by these calculations.

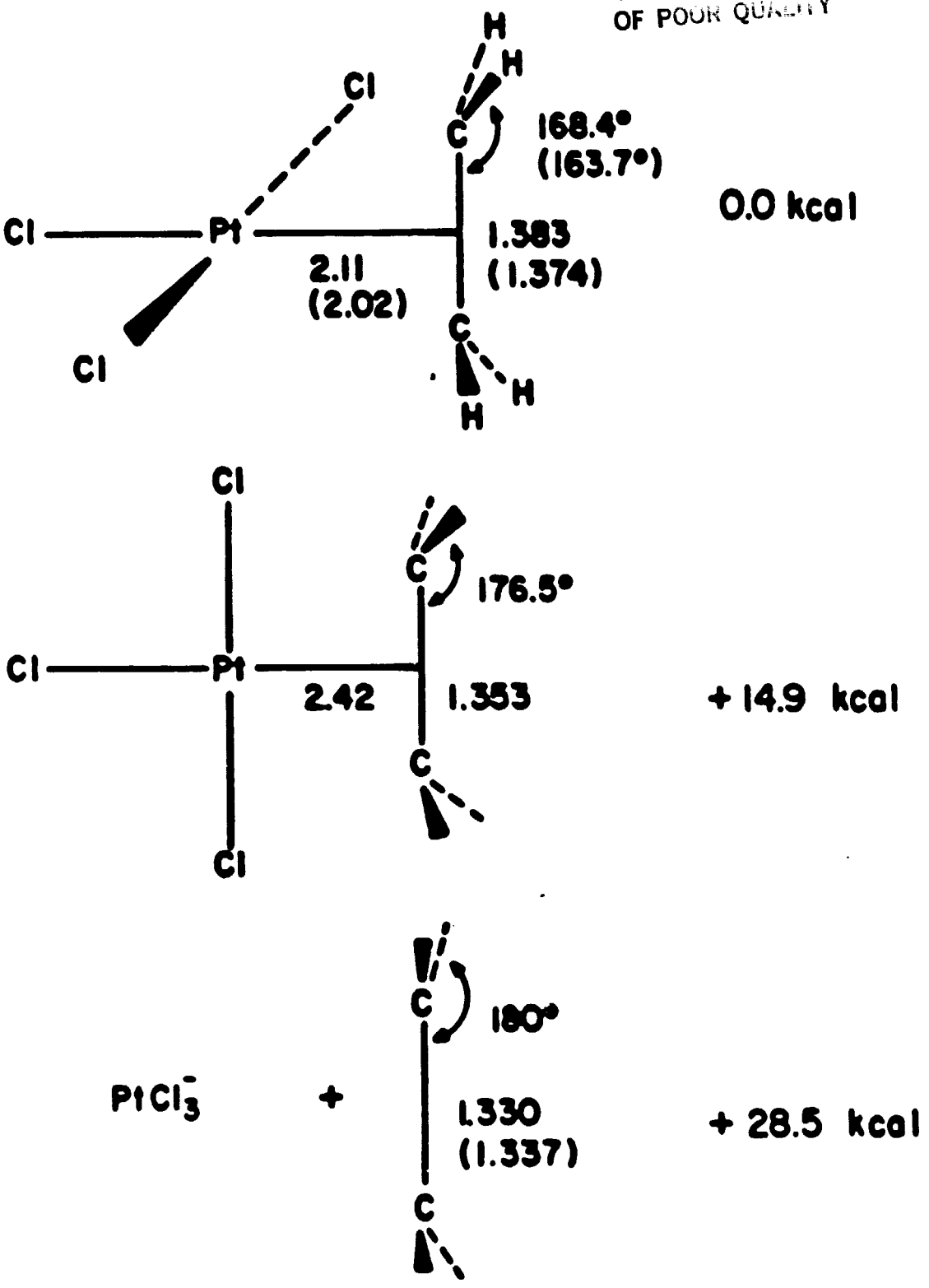

FIGURE 13. GEOMETRICAL AND ENERGETIC PARAMETERS CALCULATED BY HAY (REFERENCE 30) FOR ZEISE'S SALT, AND COMPARISON WITH EXPERIMENTALLY OBSERVED VALUES (IN PARENTHESES)

Actinide compounds have important roles in nuclear fuels, and recent attempts to develop more efficient methods to enrich uranium using lasers have focused attention on UF_6. In this connection, we carried out calculations on UF_6 to expand on the fragmentary knowledge about the nature of chemical bonding in actinide compounds.[31] We illustrate here how some of the calculated properties compared with their experimentally observed values. The bond length of UF_6 in the ground state $^1A_{1g}$ configuration was optimized. The predicted value of 3.70 bohr was found in good agreement[31] with the experimental value of 3.777 Bohr.

In Table 7 we compare the calculated excitation energies in UF_6^-, after introducing spin-orbit coupling using the simple approach defined by Equation (31), with the experimentally determined energies. The comparison is quite favorable, with the theoretical values only 0.1-0.2 eV higher in energy.[31] Table 8 compares experimental vertical ionization potentials of UF_6 with orbital energies calculated using Koopman's theorem. The orbital energies shown in this table overestimate the experimental ionization potentials by nearly 3.9 eV. Shifting the calculated values by 3.9 eV brings the calculated levels into harmony with the experimental photoelectron spectrum. Similar experiences have been found in all electron ab initio calculations on SF_6, for example. The problem is well known; it lies in the inadequacy of the delocalized molecular orbitals of the neutral molecule for describing the relaxation effects associated with the "localized hole states" of the ionized molecule. Since relaxation effects appear to alter only the absolute positions of the states of UF_6^+, an assignment could be made of the photoelectron spectrum by use of the shifted results in Table 8. The first

Table 7. Excited States of UF_6^-. Comparison of Theoretical and Experimental Results (Ref. 31)

	Excitation energy (eV)			
State	Exptl (Ref. [a])	Rel. ECP (Ref. 31)	DVM (Ref. [b])	$X\alpha$-SO (Ref. [c])
Γ_{7u}	0.00	0.00	0.00	0.00
Γ_{8u}	0.57	0.67	1.00	0.85
Γ_{7u}	0.86	0.97	1.13	1.06
Γ_{8u}	1.58	1.80	2.51	2.53
Γ_{6u}	1.77	1.95	2.69	2.50

[a] M. J. Reisfeld and G. A. Crosby, Inorg. Chem., 4, 65 (1965).

[b] D. D. Koelling, D. E. Ellis, and R. J. Bartlett, J. Chem. Phys., 65, 3331 (1976).

[c] A. M. Boring and J. H. Wood.

Table 8. Comparison of Experimental Vertical Ionization Potentials of UF_6 with calculated orbital energies(Koopmans' theorem). (ref. 31)

	Rel. HF	Rel. HF with spin–orbit coupling			Exptl[b]
$4t_{1u}$	18.43	$8u$	17.88	(13.98)[a]	13.9
		$6u$	19.11	(15.21)	15.35
$1t_{1g}$	18.56	$8g$	18.55	(14.65)	14.8
		$6g$	18.57	(14.67)	
$1t_{2u}$	19.64	$7u$	19.63	(15.73)	15.98
		$8u$	19.65	(15.75)	
$3a_{1g}$	19.73	$6g$	19.73	(15.83)	
$3t_{1u}$	20.11	$8u$	20.09	(16.19)	16.58
		$6u$	20.16	(16.26)	
$1t_{2g}$	20.58	$7g$	20.55	(16.65)	16.85
		$8g$	20.59	(16.69)	
$2e_g$	20.74	$8g$	20.74	(16.84)	17.30
$2t_{1u}$	37.76	$8u$	35.20		
		$6u$	41.95		
$2a_{1g}$	44.50	$6g$	44.50		
$1e_g$	44.71	$8g$	44.71		
$1t_{1u}$	46.44	$8u$	46.04		
		$6u$	48.56		
$1a_{1g}$	70.92	$6g$	70.92		

[a] REL. HF WITH SPIN-ORBIT COUPLING RESULTS SHIFTED BY -3.9 eV.
[b] L. KARLSSON, L. MATTSSON, R. JODRNY, T. BERGMARK, AND K. SIEGBAHN, PHYS. SCR. 14, 230 (1976).

peaks then coincide, and the remaining peaks lie no farther than 0.6 eV from a predicted ionization potential.[31]

5. SYNOPSIS

We close this part of this paper by listing the main characteristics of the method discussed here.

(1) This approach to the calculation of molecular relativistic electronic structure is based on one-component wavefunctions familiar from the nonrelativistic theory. The two principal ingredients to this approach are: (a) Cowan-Griffin relativistic Hartree-Fock atomic orbitals[6], and, (b) "relativistic" effective core potentials.[7]

(2) The relativistic effects on molecular properties of chemical interest such as the relativistic effects on the bond lengths and on the energy ordering of states appear from all cases examined to be reliably obtained by this method. The molecular wavefunctions and energies are first calculated including only the relativistic mass-velocity and Darwin terms. If the effect of spin-orbit coupling is expected to be important, then the results of the first calculation are combined with the calculation of the spin-orbit matrix. The latter is calculated using an effective one-electron spin-orbit interaction approximation. The net interaction matrix obtained in the end is diagonalized to obtain the final molecular states.

(3) This approach allows the molecular calculations to be performed by direct application of the full range of the traditional quantum chemistry techniques, including MCSCF and CI, to include electron correlation in obtaining the ground and excited states of molecules. All computational aspects of the approach that pertain to the RECP's have been tested and implemented in standard quantum chemistry programs.[13,32]

(4) This approach is applicable to polyatomic molecules of arbitrary geometry.[33] Gradient assisted RECP searches for the critical points of the potential energy surfaces of a transition metal complex have recently been reported.[34]

(5) Large computational simplifications over traditional all-electron treatments are obtained via the "relativistic" effective core potentials in their role as a device to reduce the molecular problem to just the valence electrons.

6. CRITICAL ASPECTS OF THE CONSTRUCTION OF RECP's

The reliability of the RECP's for molecular calculations rests on the properties given to the valence pseudo-orbital $\tilde{P}_{n\ell}$ through its definition, and the details thereof are thus of critical importance. Indeed, every improvement in the approach has been associated with a revision of the properties of the valence pseudo-orbital.

5.1. Linear Combination of RHF Orbitals

The traditional definition of a valence pseudo-orbital has been to take it first as a linear combination of the core and valence orbitals of the same orbital angular momentum,[35,36,12,13]

$$\tilde{P}_{nl} = \sum_{k=l+1}^{n} P_{kl} \, C_{kl,nl} \qquad 0 \leq r < \infty \tag{32}$$

The coefficients $C_{kl,nl}$ were chosen to satisfy the broad criteria given in Section 2.2. These criteria were indeed satisfied almost optimally by requiring, in the following order, that:[13]

(a) $\lim_{r \to 0} \left| \tilde{P}_{nl}/r \right| = 0$

(b) $\tilde{P}_{nl}$ be normalized

(c) $\tilde{P}_{nl}$ maximize a functional of the "smoothness" of the orbital.

The major deficiency of this definition has been found to lie in the restriction of the pseudo-orbital to the expansion given by Equation (32). Since the valence pseudo-orbital $\tilde{P}_{nl}$ is normalized, the expansion by necessity has less amplitude than the original valence orbital P_{nl} at large radial distances. The net effect is to introduce a charge redistribution into the valence space that is unphysical and can seriously impair the reliability of calculated potential energy curves. A comparison between the Hartree-Fock valence orbital and the valence pseudo-orbital is shown in Figure 14 that illustrates the charge redistribution for the case of the silicon atom 3s orbital.

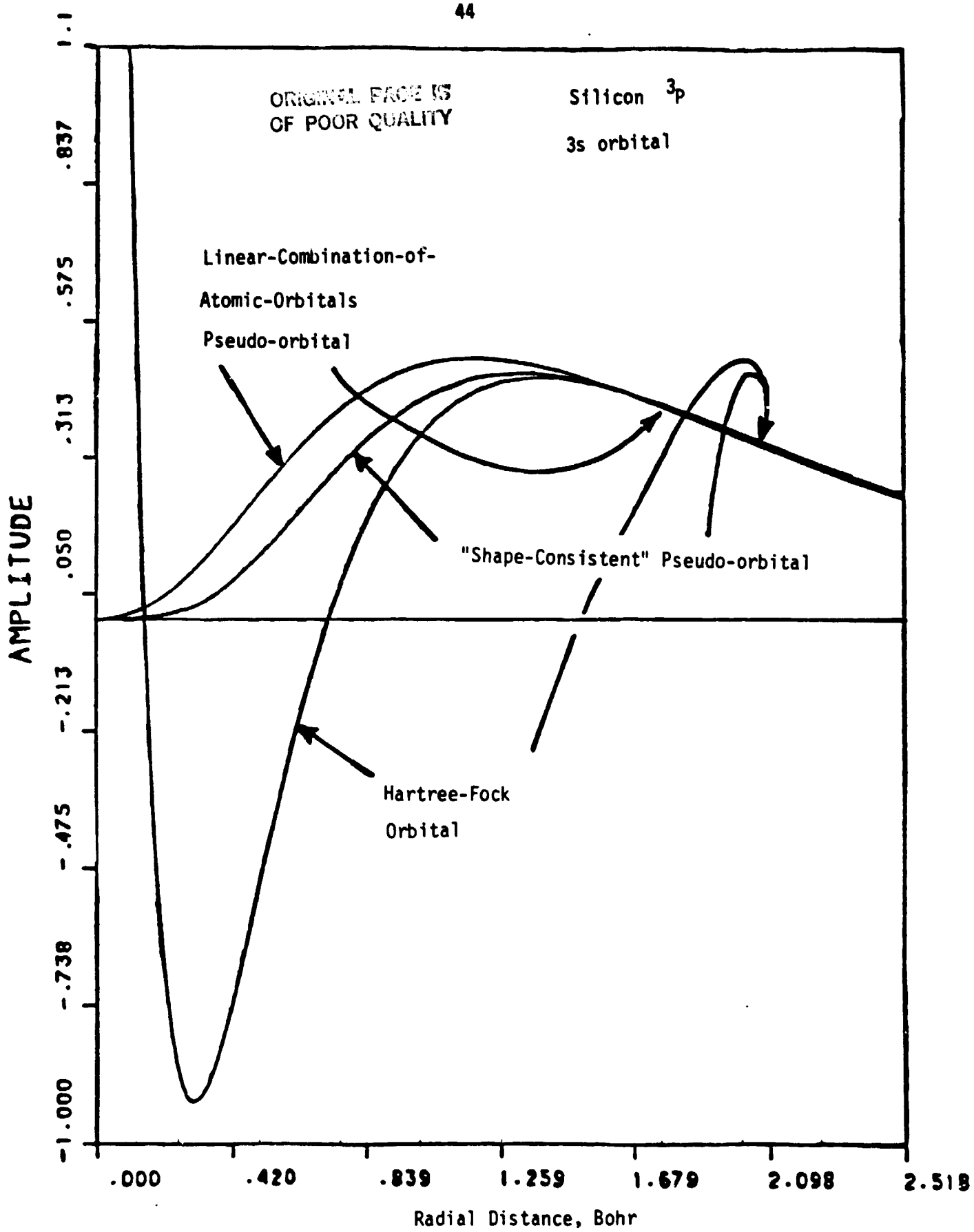

FIGURE 14. COMPARISON OF THE HARTREE-FOCK VALENCE ORBITALS WITH THE VALENCE PSEUDO-ORBITALS OF THE "LINEAR-COMBINATION-OF-ATOMIC-ORBITALS" APPROACH AND THE "SHAPE CONSISTENT" APPROACH FOR THE CASE OF THE 3s ORBITAL OF SILICON ATOM IN THE ^3P STATE

6.2. Shape-Consistent RHF Pseudo-Orbitals

The remedy to this deficiency has been found to lie in abandoning the traditional expansion, Equation (32), as a part of the valence pseudo-orbital definition. Instead, motivated by the importance of preserving the charge distribution characteristics of the original valence RHF space, the valence pseudo-orbital is first defined as identical to the RHF valence orbital over the valence segment of the orbital,[37-41]

$$\tilde{P}_{n\ell} = P_{n\ell} \qquad r \geq R_M \tag{33}$$

where R_M is a radial distance larger than the outermost node of $P_{n\ell}$, yet not much larger than the radius of the outermost valence maximum. The definition of $\tilde{P}_{n\ell}$ in the core segment of the orbital, $0 \leq r \leq R_M$, is based in turn on satisfying at least the requirements of:

(a) Nodelessness

(b) Matching of end-point (at r=0 and $r=R_M$) continuity conditions on the orbital and its derivatives (up to the third derivative at $r=R_M$)

(c) Normalization.

The core segment of $\tilde{P}_{n\ell}$ is expanded in polynomials[39], or even exponential functions.[38,41] However, only as many parameters are introduced in these expansions in practice as are required to fulfill the above listed requirements. The criterion of smoothness has not been used explicitly in this approach. Only the choice of R_M has loosely been connected in practice with the desired ultimate smoothness of $\tilde{P}_{n\ell}$.[39]

The valence pseudo-orbitals obtained by this definition are referred to as "shape-consistent" pseudo-orbitals. A typical "shape-consistent" valence pseudo-orbital is compared with the previous pseudo-orbital obtained from the linear-combination-of-atomic-orbitals definition in Figure 14 for the case of the silicon atom 3s orbital. The restoration of the proper amplitude in the valence region is shown in Figure 14 to be accompanied by a commensurate adjustment in the amplitude over the core region. Whereas the "shape-consistent" definition of valence pseudo-orbitals has been discussed by a number of workers, Christiansen, Lee, and Pitzer were the first to demonstrate the implications of the "shape-consistent" ECP's for the reliable calculation of potential energy curves.[39] One of their conclusive results for the case of the potential energy curve of the Cl_2 $X'\Sigma_g^+$ molecule is shown in Figure 15. The result of the "shape-consistent" ECP is shown in this figure to be in excellent agreement with the comparable all-electron (AE) result. In contrast, the previous ECP clearly led to a much poorer comparison.[13] Figure 15 also shows another potential energy curve in reasonable agreement with the all-electron result. This other potential energy curve was obtained by an intermediate remedy to the problem[42] that has now been superseded by "shape-consistent" approach.

6.3. Hamiltonian and Shape Consistent RHF Pseudo-Orbitals

The replacement of the RHF valence orbitals by the valence pseudo-orbitals in the valence-valence interactions causes a modification in the interactions commensurate to the modification in the orbitals. There is a

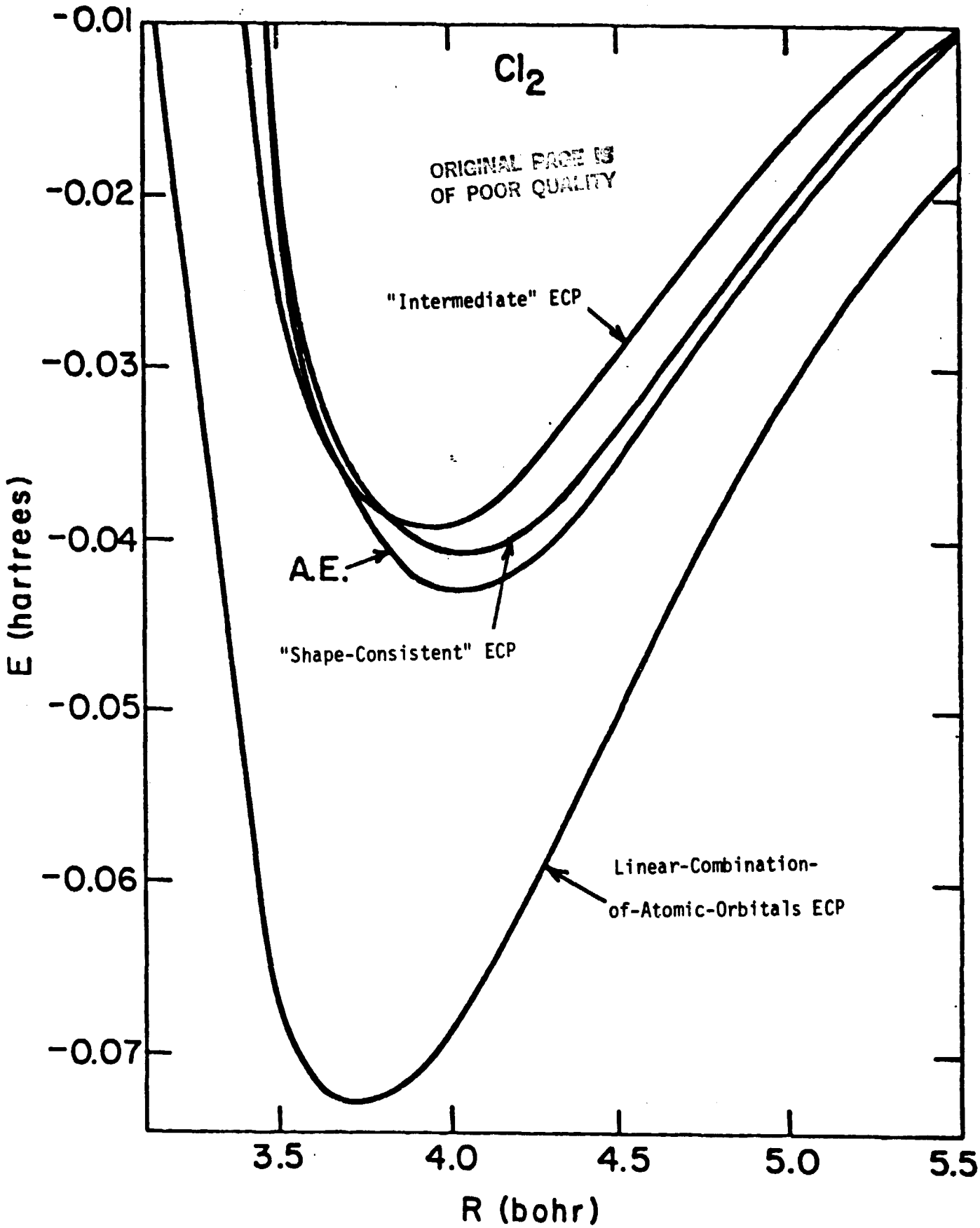

FIGURE 15. COMPARISON OF THE ALL-ELECTRON POTENTIAL ENERGY CURVE FOR THE Cl_2 MOLECULE IN THE $X'\Sigma_g^+$ STATE (CALCULATED WITH A GENERALIZED VALENCE BOND WAVEFUNCTION) WITH THE CORRESPONDING VALENCE ELECTRON RESULTS USING ECP's FROM THREE DIFFERENT APPROACHES: THE "SHAPE-CONSISTENT" APPROACH (CHRISTIANSEN, LEE, AND PITZER; REFERENCE 39), THE OLD "LINEAR-COMBINATION-OF-ATOMIC-ORBITALS" APPROACH, AND THE "INTERMEDIATE-FIX" APPROACH.

change in these important interactions even in the case of the "shape consistent" definition of the valence pseudo-orbitals. In this case, although the "shape-consistent" psuedo-orbital is identical over the valence segment with the RHF orbital, the core segment of the pseudo-orbital only satisfies the normalization condition among all the important other orbital properties that determine the valence-valence interactions. Rappé, Smedley, and Goddard have proposed to enhance the definition of the core segment of the valence pseudo-orbital so as to minimize the remaining error in the valence-valence interactions.[43] This enhanced definition of the valence pseudo-orbitals is referred to as the "hamiltonian and shape consistent" approach.

6.4. The Method of Moment-Accumulation Functions: A New Approach

The minimization of the error in the valence-valence interactions supplies important additional conditions for the definition of the core segment of the valence pseudo-orbital. However, the relationship between the satisfaction of this criterion and the requisite characteristics of the individual core segments of the valence pseudo-orbitals is complex and indirect. We show below a new approach whereby the specific orbital properties that affect the minimization of the error in the valence-valence interactions can be isolated from the peripheral intricacies of the energy interactions.[44] In fact, these new specific orbital properties are found to constitute a set of conditions on the individual orbitals of the same simplicity as the normalization condition.[44]

The sum of the valence-valence interactions is contained in the atomic valence energy. The atomic valence energy is given by[45]

$$E^{VAL.} = \sum_{n\ell \in \underset{\sim}{V}} O_{n\ell} I_{n\ell} + \delta E^{VAL.}$$
$$+ \sum_{n\ell \in \underset{\sim}{V}} \frac{O_{n\ell}(O_{n\ell}-1)}{2} \left[F^0(n\ell,n\ell) - \frac{2\ell+1}{4\ell+1} \sum_{\lambda=2,2}^{2\ell} A_\lambda(\ell,\ell) F^\lambda(n\ell,n\ell) \right]$$
$$+ \sum\sum_{n\ell \in \underset{\sim}{V} > n'\ell' \in \underset{\sim}{V}} O_{n\ell} O_{n'\ell'} \left[F^0(n\ell,n'\ell') - \frac{1}{2} \sum_{\lambda=|\ell-\ell'|,2}^{\ell+\ell'} A_\lambda(\ell,\ell') G^\lambda(n\ell,n'\ell') \right] \quad (34)$$

The terms in this expression range only over the set of valence orbitals $\{P_{n\ell}\}$, denoted as $\underset{\sim}{V}$. The orbital occupation numbers are denoted $Q_{n\ell}$, while the $A_\lambda(\ell,\ell')$ coefficients are the Roothaan vector coupling coefficients[46]; the latter are simply related to the Clebsh-Gordan coefficients. The $I_{n\ell}$ terms are one-electron integrals of the effective one-electron operator containing the RECP. The term δE^{VAL} stands for the deviation of the multiplet energy from the average energy of configurations. This energy contribution introduces only additional combinations of the type of interactions already present, and its detailed structure is therefore of no importance here.

The two-electrons interactions among the atomic valence orbitals are given by the well known F and G integrals. These interactions are defined by[45]

$$F^\lambda(n\ell,n'\ell') = \int_0^\infty \int_0^\infty P_{n\ell}(r) P_{n'\ell'}(r') \frac{r_<^\lambda}{r_>^{\lambda+1}} P_{n\ell}(r) P_{n'\ell'}(r') \, dr \, dr' \quad (35a)$$

and

$$G^\lambda(n\ell,n'\ell') = \int_0^\infty \int_0^\infty P_{n\ell}(r) P_{n'\ell'}(r') \frac{r_<^\lambda}{r_>^{\lambda+1}} P_{n\ell}(r') P_{n'\ell'}(r) \, dr \, dr' \quad (35b)$$

In this traditional form, the properties of the core segment of the valence pseudo-orbital are interwoven in the intricacies of the energy expression, E^{VAL}, and no discrete succinct measures of the valence pseudo-orbital characteristic can be seen to relate to the minimization of the error in the valence-valence interactions.

We show next a new expression for the formula of the F and G integrals that does indeed bear out through these integrals the dependence of the valence-valence interaction on a set of discrete succinct measures of orbital characteristics. We define the function

$$Q^{\lambda}_{n\ell,n'\ell'}(r) \equiv \int_0^r P_{n\ell}(t)\, t^{\lambda}\, P_{n'\ell'}(t)\, dt \quad , \quad 0 \leq r < \infty \qquad (36)$$

We shall name this orbital characteristic the "moment accumulation" function. These functions become the various λ-order transition moments of the valence set of functions as the radial distance from the nucleus approaches infinity. The special case of the function $Q^{0}_{n\ell,n\ell}(r)$ describes the physical increase in the amount of charge deriving from the $P_{n\ell}(r)$ orbital as the radial distance from the nucleus increases; we refer to it as "charge accumulation" function. In particular

$$\lim_{\lambda \to \infty} Q^{0}_{n\ell,n\ell}(r) = 1 \qquad (37)$$

because of the normalization of the radial functions. Analogously,

$$\lim_{r \to \infty} Q^{\circ}_{n\ell,n'\ell}(r) = 0 \qquad (38)$$

because of the orthonormality of the radial functions.

The function $Q^{o}_{n\ell,n\ell}(r)$ first serves to clearly bring out the nature of the improvement of the orbital properties brought about by the "shape consistent" pseudo-orbital definition. Figure 16 shows a comparison of the $Q^{o}_{3s,3s}(r)$ function deriving from the Hartree-Fock valence orbitals with those deriving from the valence pseudo-orbitals for the case of the 3s orbital of silicon atom. Apart from an expected small discrepancy in the core region, the "shape consistent" 3s pseudo-orbital leads to an exact match with the Hartree-Fock charge distribution over the whole valence region. The overall improvement in the charge distribution over that obtained from the older pseudo-orbital deriving from the linear-combination-of-atomic-orbitals definition is shown in Figure 16. The latter pseudo-orbital yields a charge distribution that differs from the Hartree-Fock distribution not only over the core region but over a large part of the valence region.

We note, as a digression, that the "charge accumulation" function, $Q^{o}_{3s,3s}(r)$, serves also to give a measure of the onset of the physically meaningful valence segment of a valence orbital. The outermost maximum of the 3s orbital is shown in Figure 14 to be at about r=1.26 Bohr. This point might perhaps be interpreted as already in the midst of what one would call the

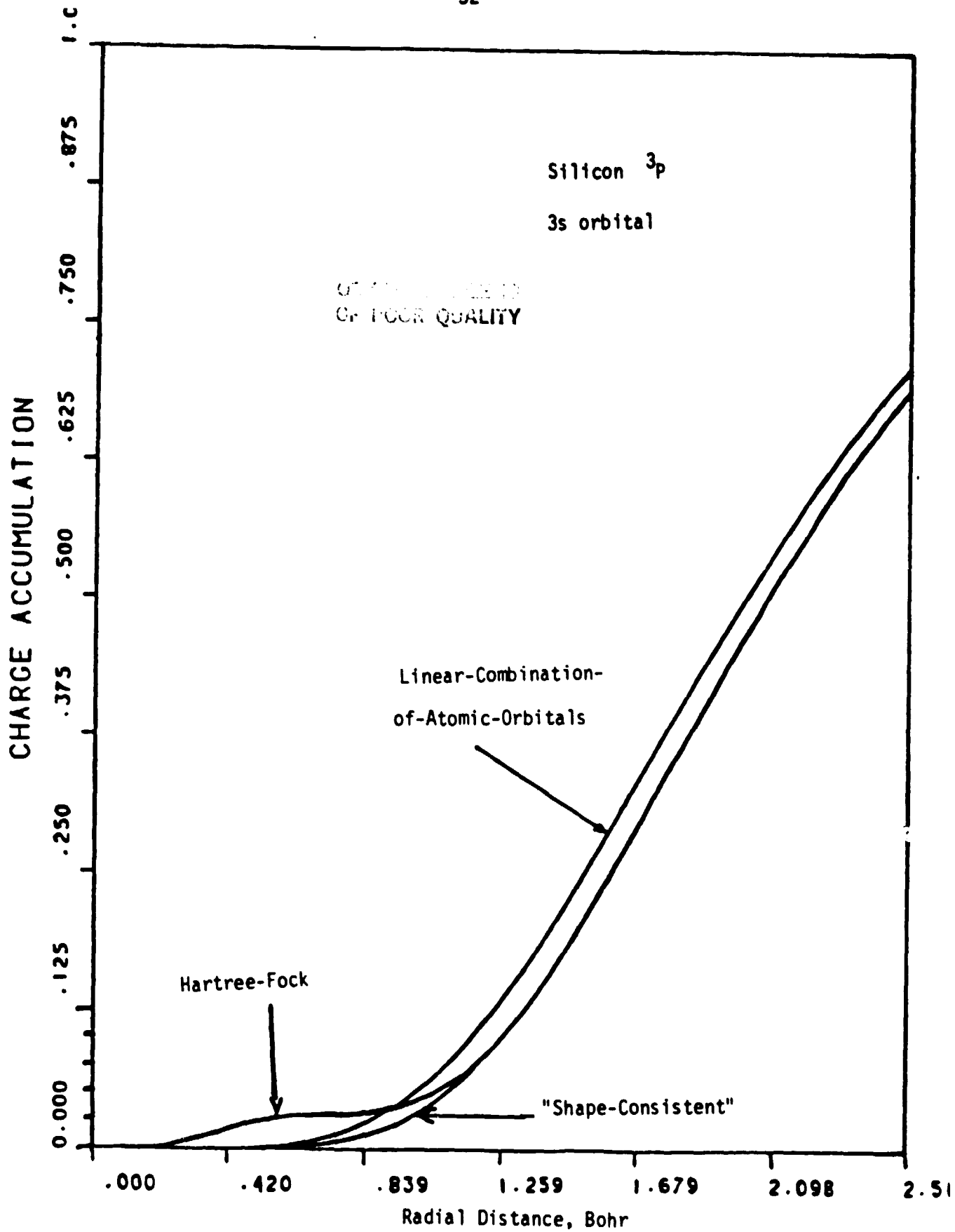

FIGURE 16. COMPARISON OF THE CHARACTERISTICS OF THE "CHARGE ACCUMULATION" FUNCTION OF THE HARTREE-FOCK 3s ORBITAL OF SILICON ATOM, AS A FUNCTION OF RADIAL DISTANCE, WITH THE "CHARGE ACCUMULATION" FUNCTION OBTAINED FROM THE VALENCE PSEUDO-ORBITALS OF THE "SHAPE-CONSISTENT" APPROACH AND THE OLD "LINEAR-COMBINATION-OF-ATOMIC-ORBITALS" APPROACH

physically meaningful valence region. We note, however, that Figure 16 shows the amount of charge accumulated up to this outermost maximum, at r=1.26 Bohr, to be only about .05, 5% of the total charge.

The properties of the "charge accumulation" function are also directly related to the basic electrostatic interactions among the electrons. The traditional expression for the Coulomb potential with the 3s orbital density as its source is

$$J(\underset{\sim}{r}) = \frac{1}{4\pi} \int \frac{[P_{3s}(r')/r']^2}{\|\underset{\sim}{r} - \underset{\sim}{r}'\|} d\underset{\sim}{r}' \tag{39}$$

Carrying out the angular integrations yields the well known formula

$$J(r) = \frac{1}{r} \int_0^r P_{3s}^2(t)\, dt + \int_r^\infty P_{3s}^2(t) \frac{1}{t}\, dt \tag{40}$$

The contribution of the P_{3s} orbital is spread out over two distinct terms in this expression. Integrating by parts, however, we find that both terms can be consolidated into a single term that depends concisely on P_{3s} through the "charge accumulation" function, $Q^0_{3s,3s}(r)$. We obtain

$$J(r) = \int_r^\infty \frac{Q^0_{3s,3s}(t)}{t^2}\, dt \tag{41}$$

The asymptotic expansion of the above expression for the Coulomb potential for large r yields the well-known point charge-like expression

$$v^{*}(r) \xrightarrow[\text{large } r]{} \frac{Q^{*}_{3s,3s}(r)}{r} \tag{42}$$

This illustrates the central role that the orbital properties contained in the charge accumulation function have in the basic electrostatic interactions among electrons.

Figure 17 shows a comparison of the Coulomb potentials resulting from the three different "charge accumulation" functions shown previously in Figure 16. The Coulomb potential deriving from the "shape-consistent" valence pseudo-orbital is seen to agree perfectly in the valence region with the potential derived from the Hartree-Fock orbital. In contrast, the pseudo-orbital deriving from the linear-combination-of-atomic-orbitals definition yields a Coulomb potential that, consistent with the corresponding "charge-accumulation" function shown in Figure 16, is too repulsive even in the valence region of the valence orbital.

Indeed, the F and G integrals themselves may be reexpressed in terms of the "moment accumulation" functions. Starting from the definition given by Equations (35a) and (35b), and integrating by parts repeatedly, we find that

$$F^{\lambda}(n\ell,n'\ell') = (2\lambda+1)\int_0^{\infty} Q^{\lambda}_{n\ell,n\ell}(t)\, Q^{\lambda}_{n'\ell',n'\ell'}(t)\, \frac{1}{t^{2\lambda+2}}\, dt \tag{43a}$$

and

$$G^{\lambda}(n\ell,n'\ell') = (2\lambda+1)\int_0^{\infty} \left[Q^{\lambda}_{n\ell,n'\ell'}(t)\right]^2 \frac{1}{t^{2\lambda+2}}\, dt \tag{43b}$$

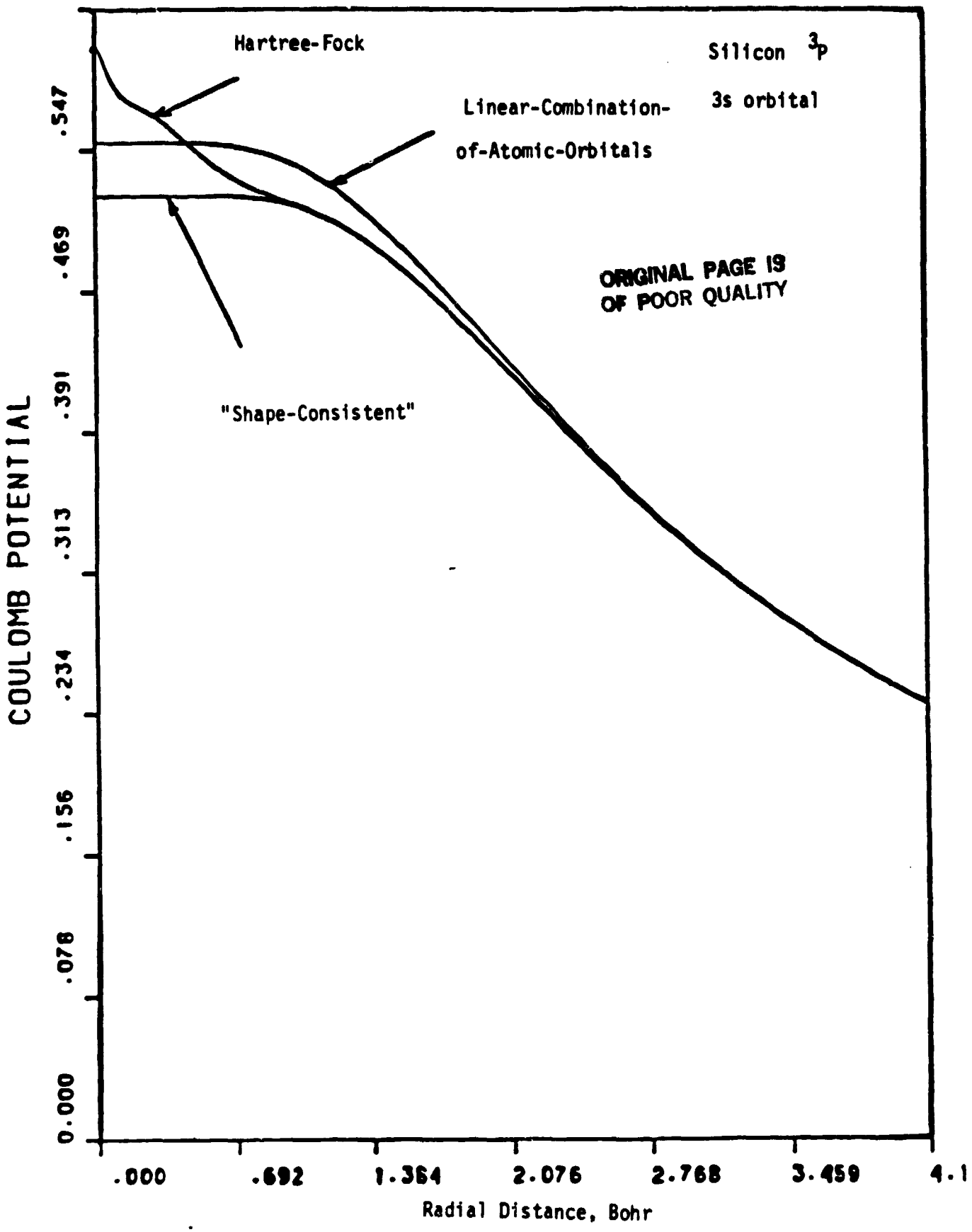

FIGURE 17. COMPARISON OF THE CHARACTERISTICS OF THE COULOMB POTENTIAL, AS A FUNCTION OF RADIAL DISTANCE, OBTAINED FROM THE DENSITY OF THE HARTREE-FOCK 3s ORBITAL OF SILICON ATOM WITH THE COULOMB POTENTIAL OBTAINED FROM THE VALENCE PSEUDO-ORBITALS OF THE "SHAPE CONSISTENT" APPROACH AND THE OLD "LINEAR-COMBINTATION-OF-ATOMIC-ORBITAL" APPROACH

This proves that through these expressions for the F and G integrals, the valence-valence interaction in E^{VAL}, Equation (34), depends on the valence pseudo-orbital properties embodied in the set of "moment accumulation" functions.

It follows that minimization of the error in the valence-valence interaction is equivalent to the requirement that the core-segment of the valence pseudo-orbitals in the "shape consistent" definition satisfy the Hartree-Fock values of

$$\left\{ Q^{\lambda}_{n\ell,n\ell}(R_M) \, , \; \lambda = 0,2,\ldots,2\ell \right\} \quad , \quad n\ell \in \underset{\sim}{V} \tag{44a}$$

and

$$\left\{ Q^{\lambda}_{n\ell,n'\ell'}(R_M) \, , \; \lambda = |\ell-\ell'|, \ell+\ell', 2 \right\} \quad , \; n\ell \in \underset{\sim}{V} > n'\ell' \in \underset{\sim}{V} \tag{44b}$$

This set of conditions contains the normalization conditions,

$$\left\{ Q^{0}_{n\ell,n\ell}(R_M) \right\} \quad , \quad n\ell \in \underset{\sim}{V} \tag{45}$$

as a subset. The replacement of the single condition of normalization by the above "moment accumulation" set of conditions appears to provide the most natural transition from the "shape-consistent" into the "hamiltonian

and shape consistent" approach. Indeed, the increase of the required set of "moment accumulation" functions beyond Equation (44) provides a systematic procedure for the definition of pseudo-orbitals that increasingly tend to the original Hartree-Fock valence orbitals and is independent of the availability of a pertinent energy expression. The limit is, of course, inconsistent with the desired criterion of nodelessness in the definitions of valence pseudo-orbitals, and is, therefore, primarily of interest as a generalization of the approach.

The transition from the "normalization" condition to the "moment accumulation" conditions in the "shape-consistent" approach requires an extension of the form of the expansion of the core segment of the valence pseudo-orbital. Rather than simply expand in a single continuous polynomial of increasingly higher degree, it appears to be preferable to expand in a large number (possibly simulating a complete basis) of piece-wise continuous polynomials such as, for example, cubic splines of finite support. Moreover, the condition of "smoothness" of the valence pseudo-orbital can simply be added to determine all degrees of freedom in the expansion not fixed by the "moment-accumulation" conditions. This provides a systematic procedure for obtaining valence pseudo-orbitals wherein the final form of the resulting RECP's is independent of constraints on its shape that may result from an expression for the core segment of the valance pseudo-orbital with just a minimal set of parameters. Finally, we note that the "moment accumulation" conditions include conditions that couple the various valence pseudo-orbitals. The satisfaction of the "moment accumulation" conditions hence requires that all the valence pseudo-orbitals be solved simultaneously. In contrast, the old "shape-consistent" procedure allowed each valence pseudo-orbital to be obtained independently since no recognition was given to the interdependence of these orbitals.

7. THE LONG-RANGE BEHAVIOR OF THE RECP: A NEW ANALYSIS

The characteristics of the long-range segment of the RECP's have been shown to be an important factor in the reliability with which molecular potential energy curves can be calculated using the RECP's.[42] This interdependence is not surprising in view of the large overlap between the long-range segment of the RECP's and the electron densities of neighboring atoms at equilibrium internuclear distances. Atomic calculations, in contrast, provide almost no test of the long-range properties of the RECP's because of the small overlap of the atomic charge density with the long-range segment of the RECP.

We present next the first detailed analysis in terms of moment accumulation functions of the characteristics of the long-range behavior of RECP's. Starting from the expression for the RECP given in Equation (18), and using the properties of the $P_{n\ell}$ orbitals, one obtains

$$U_\ell(r) = \frac{U_{n\ell}^{CORE} P_{n\ell}}{P_{n\ell}} + \frac{\left(U_{n\ell}^{VAL.} P_{n\ell} - \tilde{U}_{n\ell}^{VAL} \tilde{P}_{n\ell} \right)}{P_{n\ell}} \qquad (46)$$

for $r \geq R_M$. The first term is the local core-valence interaction, and the second term is the local residual in the valence-valence interactions. These terms consist of radial Coulomb and exchange potentials, the general form of which is traditionally given in terms of the Y functions. The latter are defined as

$$Y^\lambda_{n\ell,n'\ell'}(r) = \frac{1}{r^\lambda} \int_0^r P_{n\ell}(t) t^\lambda P_{n'\ell'}(t)\, dt + r^{\lambda+1} \int_r^\infty P_{n\ell}(t) \frac{1}{t^{\lambda+1}} P_{n'\ell'}(t)\, dt \qquad (47)$$

We first obtain an alternative expression for the Y functions in terms of "moment accumulation" functions,

$$Y^{\lambda}_{n\ell,n'\ell'}(r) = (2\lambda+1)\, r^{\lambda+1} \int_r^{\infty} Q^{\lambda}_{n\ell,n'\ell'}(t)\, \frac{1}{t^{2\lambda+2}}\, dt \ , \tag{48}$$

by integration by parts.

We first analyze the residual of the valence-valence interactions. Using the expressions for the Coulomb and exchange potentials in terms of the "moment accumulation" function, we obtain

$$\begin{aligned}\left(\frac{U^{VAL}_{n\ell} P_{n\ell} - \tilde{U}^{VAL}_{n\ell} \tilde{P}_{n\ell}}{P_{n\ell}} \right) = (Q_{n\ell} - 1) \Bigg\{ & \int_r^{\infty} \left[Q^{0}_{n\ell,n\ell}(t) - \tilde{Q}^{0}_{n\ell,n\ell}(t) \right] \frac{1}{t^2}\, dt \\ & + \frac{2\ell+1}{4\ell+1} \sum_{\lambda=2,2}^{2\ell} (2\lambda+1)\, A_{\lambda}(\ell,\ell)\, r^{\lambda} \int_r^{\infty} \left[\tilde{Q}^{\lambda}_{n\ell,n\ell}(t) - Q^{\lambda}_{n\ell,n\ell}(t) \right] \frac{1}{t^{2\lambda+2}}\, dt \Bigg\} \\ & + \sum_{\substack{n'\ell' \in V \\ n'\ell' \neq n\ell}} Q_{n'\ell'} \Bigg\{ \int_r^{\infty} \left[Q^{0}_{n'\ell',n'\ell'}(t) - \tilde{Q}^{0}_{n'\ell',n'\ell'}(t) \right] \frac{1}{t^2}\, dt \\ & + \frac{1}{2} \sum_{\lambda=|\ell-\ell'|,2}^{\ell+\ell'} (2\lambda+1)\, A_{\lambda}(\ell,\ell')\, r^{\lambda} \left(\frac{P_{n'\ell'}}{P_{n\ell}} \right) \int_r^{\infty} \left[\tilde{Q}^{\lambda}_{n'\ell',n\ell}(t) - Q^{\lambda}_{n'\ell',n\ell}(t) \right] \frac{dt}{t^{2\lambda+2}} \Bigg\} \end{aligned} \tag{49}$$

The residual of the valence-valence interactions is seen to depend on the <u>difference</u> between the "moment accumulation" functions calculated from the valence RHF orbitals and from the valence pseudo-orbitals (indicated by a superscript tilde). We have restricted the expression for the valence-valence interaction to the case of the average-energy-of-configurations since it suffices to illustrate the long-range characteristics of the RECP.

The core segment of the valence pseudo-orbital of the "shape-consistent" approach satisfies the normalization condition

$$\tilde{Q}^{0}_{n\ell,n\ell}(R_M) = Q^{0}_{n\ell,n\ell}(R_M) \quad , \; n\ell \in \underset{\sim}{V} \tag{50}$$

Consequently, in the "shape-consistent" approach the first and third terms of the residual in the valence-valence interaction, Equation (49), are zero. However, the remaining terms in the residual of the valence-valence interactions are not equal to zero for "shape consistent"-only orbitals. In the "moment accumulation" formulation of the "hamiltonian and shape consistent" approach, we require that the core segment of the valence pseudo-orbital satisfy the full set of conditions

$$\tilde{Q}^{\lambda}_{n\ell,n\ell}(R_M) = Q^{\lambda}_{n\ell,n\ell}(R_M) \quad , \; \lambda = 0,2,\ldots,2\ell \; ; \; n\ell \in \underset{\sim}{V} \tag{51a}$$

$$\tilde{Q}^{\lambda}_{n\ell,n'\ell'}(R_M) = Q^{\lambda}_{n\ell,n'\ell'}(R_M) \quad , \; \lambda = |\ell-\ell'|, \ell+\ell', 2 \; ; \; n\ell \in \underset{\sim}{V} > n'\ell' \in \underset{\sim}{V} \tag{51b}$$

It follows from Equation (49) that in the "hamiltonian and shape consistent" approach the full residual in the valence-valence interactions vanishes for $r \geq R_M$, i.e.,

$$\frac{\left| U_{n\ell}^{VAL} P_{n\ell} - \tilde{U}_{n\ell}^{VAL} \tilde{P}_{n\ell} \right|}{P_{n\ell}} = 0 \qquad r \geq R_M \tag{52}$$

The RECP is therefore reduced to the local core-valence interaction,

$$U_\ell(r) = \frac{U_{n\ell}^{CORE} P_{n\ell}}{P_{n\ell}} \qquad r \geq R_M \tag{53}$$

provided the moment accumulation conditions given by Equation (51) are satisfied. Expressing the Coulomb and exchange interactions in terms of "moment accumulation" functions, we obtain for $r \geq R_M$

$$U_\ell(r) = \sum_{n'\ell' \in \underset{\sim}{C}} (2\ell'+1) \left\{ 2 \int_r^\infty Q^\bullet_{n'\ell',n'\ell'}(t) \frac{1}{t^2} dt \right.$$

$$\left. - \sum_{\lambda=|\ell-\ell'|,2}^{\ell+\ell'} (2\lambda+1) A_\lambda(\ell,\ell') r^\lambda \left(\frac{P_{n'\ell'}}{P_{n\ell}} \right) \int_r^\infty Q^\lambda_{n'\ell',n\ell}(t) \frac{1}{t^{2\lambda+2}} dt \right\} \tag{54}$$

The set of all core orbitals is denoted as $\underset{\sim}{C}$.

Finally, we discuss the long-range behavior for $r \gg R_M$. The asymptotic expansion of the Y functions for large radial distances yields

$$Y^\lambda_{n\ell,n'\ell'}(r) \sim \frac{1}{r^\lambda} Q^\lambda_{n\ell,n'\ell'}(r) \qquad r \gg R_M \tag{55}$$

In turn, the asymptotic expansion of the RECP for large radial distances is

$$U_\ell(r) \sim \frac{N_c}{r} - \sum_{n'\ell' \in \underline{C}} (2\ell'+1) \sum_{\lambda=|\ell-\ell'|,2}^{\ell+\ell'} A_\lambda(\ell,\ell') \frac{Q^\lambda_{n\ell,n'\ell'}(r)}{r^{\lambda+1}} \left(\frac{P_{n'\ell'}}{P_{n\ell}}\right) \qquad (56)$$

under the assumption that the residual in the valence-valence interactions is zero. The leading term is the point-charge potential N_c/r where N_c is the number of core electrons. This is indeed in accord with what is expected on physical grounds. If the core segment of the valence pseudo-orbital only satisfies the normalization condition, then the residual in the valence-valence interactions unfortunately also contributes a term to the long-range interaction. We find in that case that, for $r \gg R_M$,

$$\frac{\left(U^{VAL}_{n\ell} P_{n\ell} - \tilde{U}^{VAL}_{n\ell} \tilde{P}_{n\ell}\right)}{P_{n\ell}} \sim (O_{n\ell}-1) \frac{2\ell+1}{4\ell+1} \sum_{\lambda=2,2}^{2\ell} A_\lambda(\ell,\ell) \frac{1}{r^{\lambda+1}} \left[\tilde{Q}^\lambda_{n\ell,n\ell}(r) - Q^\lambda_{n\ell,n\ell}(r)\right]$$

$$+ \frac{1}{2} \sum_{\substack{n'\ell' \in \underline{V} \\ n'\ell' \neq n\ell}} O_{n\ell} \sum_{\lambda=|\ell-\ell'|,2}^{\ell+\ell'} A_\lambda(\ell,\ell') \frac{1}{r^{\lambda+1}} \left[\tilde{Q}^\lambda_{n'\ell',n\ell}(r) - Q^\lambda_{n'\ell',n\ell}(r)\right] \left(\frac{P_{n'\ell'}}{P_{n\ell}}\right) \qquad (57)$$

This long-range contribution, however, is clearly an artifact of the insufficient definition of the valence pseudo-orbital.

8. ACKNOWLEDGMENTS

I wish to thank Dr. Jeff Hay for his kind help in gathering much of the needed information for this paper. Support of part of this work by NASA-Ames Research Center under Grant NSG-2027 is gratefully acknowledged.

REFERENCES

(1) B. Swirles, Proc. R. Soc. (London) Ser. A 152, 625 (1935).

(2) I. P. Grant, Proc. R. Soc. (London) Ser. A 262, 555 (1961).

(3) J. P. Desclaux, D. F. Mayers, and F. O'Brien, J. Phys. B 4, 631 (1971); J. P. Desclaux, At. Data 12, 311 (1973); J. P. Desclaux and P. Pyykkö, Chem. Phys. Lett. 29, 534 (1974); 39, 300 (1976); P. Pyykkö and J. P. Desclaux, Chem. Phys. Lett. 42, 545 (1976); Nature 266, 336 (1977); Chem. Phys. Lett. 50, 503(1977); 34, 261 (1978).

(4) Y. S. Lee, W. C. Ermler, and K. S. Pitzer, J. Chem. Phys. 67, 5861 (1977).

(5) P. Hafner and W.H.E. Schwarz, J. Phys. B 11, 217, 2975 (1978); Chem. Phys. Lett. 65, 537 (1979); P. Hafner, P. Habitz, Y. Ishikawa, E. Wechsel-Trakowski, and W.H.E. Schwarz, Chem. Phys. Lett. 80, 311 (1981).

(6) R. D. Cowan and D. C. Griffin, J. Opt. Soc. Am. 66, 1010 (1976).

(7) L. R. Kahn, P. J. Hay, and R. D. Cowan, J. Chem. Phys. 68, 2386 (1978).

(8) R. D. Cowan, Phys. Rev. 163, 54 (1967).

(9) P. J. Hay, W. R. Wadt, L. R. Kahn, and F. W. Bobrowicz, J. Chem. Phys., 69, 984 (1978).

(10) W. A. Goddard,III, Phys. Rev. 174, 659 (1968).

(11) L. R. Kahn and W. A. Goddard, III, Chem. Phys. Lett. 2, 667 (1968); J. Chem. Phys. 56, 2685 (1972).

(12) C. F. Melius and W. A. Goddard, III, Phys. Rev. A 10, 1528 (1974).

(13) L. R. Kahn, P. Baybutt, and D. G. Truhlar, J. Chem. Phys. 65, 3826 (1976).

(14) C. F. Melius, B. D. Olafson, and W. A. Goddard,III, Chem. Phys. Lett. 28, 457 (1974).

(15) J. S. Cohen and B. Schneider, J. Chem. Phys. 61, 3230 (1974).

(16) W. R. Wadt, P. J. Hay, and L. R. Kahn, J. Chem. Phys. 68, 1752 (1978).

(17) J. S. Cohen, W. R. Wadt, and P. J. Hay, J. Chem. Phys. 71, 2955 (1979).

(18) H. A. Bethe and E. E. Salpeter, Quantum Mechanics of One-and Two-Electron Atoms (Springer Verlag, Berlin, 1957).

(19) S. R. Langhoff and C. W. Kern, "Molecular Fine Structure", in Methods of Electronic Structure Theory, edited by H. F. Schaefer III (Plenum, New York, 1977), Chap. 10.

(20) L. E. McMurchie and E. R. Davidson, J. Comput. Phys. 26, 218 (1978).

(21) S. R. Langhoff, J. Chem. Phys. 61, 1708 (1974).

(22) S. R. Langhoff, J. Chem. Phys. 73, 2379 (1980).

(23) P. G. Lykos and R. G. Parr, J. Chem. Phys. 24, 1166 (1956).

(24) L. R. Kahn, unpublished work.

(25) W. C. Ermler, Y. S. Lee, P. A. Christiansen, and K. S. Pitzer, Chem. Phys. Lett. 81, 70 (1981).

(26) W. J. Stevens and M. Krauss, Chem. Phys. Lett. 86, 320 (1982); J. Chem. Phys. 76, 3834 (1982).

(27) W. R. Wadt, "An Approximate Method to Incorporate Spin-Orbit Effects Into Calculations Using Effective Core Potentials", Chem. Phys. Lett. (in press).

(28) T. Ziegler, J. G. Snijders and E. J. Baerends, J. Chem. Phys. 74, 1271 (1981).

(29) M.L.H. Green, Organometallic Compounds. The Transition Elements, Vol. 2 (Methuen, London, 1968).

(30) P. J. Hay, J. Am. Chem. Soc. 103, 1390 (1981).

(31) P. J. Hay, W. R. Wadt, L. R. Kahn, R. C. Raffenetti, and D. H. Phillips, J. Chem. Phys. 71, 1767 (1979).

(32) L. E. McMurchie and E. R. Davidson, J. Comput. Phys. 44, 289 (1981).

(33) P. Baybutt, F. W. Bobrowicz, L. R. Kahn, and D. G. Truhlar, J. Chem. Phys. 68, 4809 (1978); R. J. Bartlett, L. R. Kahn, and G. D. Purvis, J. Chem. Phys. 76, 731 (1982).

(34) K. Kitaura, S. Obara, and K. Morokuma, Chem. Phys. Lett. 77, 452 (1981).

(35) J. C. Phillips and L. Kleinman, Phys. Rev. 116, 287 (1959).

(36) L. Szasz and G. McGinn, J. Chem. Phys. 42, 2363 (1965); 45, 2898 (1966).

(37) Ph. Durand and J. C. Barthelat, Theoret. Chim. Acta 38, 283 (1975).

(38) A. Redondo, W. A. Goddard, III, and T. C. McGill, Phys. Rev. B 15, 5038 (1977).

(39) D. Christiansen, Y. S. Lee, and K. S. Pitzer, J. Chem. Phys. 71, 4495 (1979).

(40) D. R. Hamann, M. Schluter, and C. Chiang, Phys. Rev. Lett. 43, 1494 (1979).

(41) A. Zunger, J. Vac. Sci. Tech. 16, 1337 (1979).

(42) P. J. Hay, W. R. Wadt, and L. R. Kahn, J. Chem. Phys. 68, 3059 (1978).

(43) A. K. Rappé, T. A. Smedley, and W. A. Goddard, III, J. Phys. Chem. 85, 1662 (1981).

(44) L. R. Kahn, unpublished work.

(45) J. C. Slater, Quantum Theory of Atomic Structure, Vols. I and II, (McGraw-Hill, New York, 1960).

(46) C.C.J. Roothaan, L. M. Sachs, and A. W. Weiss, Rev. Mod. Phys. 32, 1861 (1960).

FIGURE CAPTIONS

Figure 1. Comparison of the non-relativistic (NR) and relativistic (R) Hartree-Fock 7s orbitals in uranium atom.

Figure 2. Comparison of the non-relativistic (NR) and relativistic (R) Hartree-Fock 5f orbitals in uranium atom.

Figure 3. A nodeless 2s orbital in lithium atom, ϕ_{2s}^{Gl}, and the corresponding nodeful 2s Hartree-Fock orbital.

Figure 4. The s, p, and d local effective core potentials for the lithium atom.

Figure 5. Schematic representation of the one-electron orbital spectrum associated with the s, p, and d local effective core potentials for the Lithium atom, respectively.

Figure 6. Comparison of a valence molecular orbital for LiH $X'\Sigma^+$ obtained from the valence electron (VE) ECP calculation and a comparable all-electron (AE) calculation.

Figure 7. Comparison of the valence molecular orbital for Li_2^+ $X^2\Sigma_g^+$ obtained from the valence electron (VE) ECP calculation and a comparable all-electron (AE) calculation.

Figure 8. Schematic comparison of two possible valence pseudo-orbitals, $\tilde{P}_{n\ell}$, with the parent Hartree-Fock valence orbital, $P_{n\ell}$.

Figure 8. Schematic comparison of two possible valence pseudo-orbitals, $\tilde{P}_{n\ell}$.

Figure 9. Comparison of the nonrelativistic (NR) and relativistic (R) valence electron (VE) potential energy curves for the low-lying electronic states of the XeF molecule prior to the inclusion of the spin-orbit effects.

Figure 10. The relativistic (R) valence electron (VE) potential energy curves for the low-lying electronic states of the XeF molecule including spin-orbit effects (using the atoms-in-molecules approximation).

Figure 11. Spin-orbit coupling matrix elements between electronic states of the rare gas oxides computed by Langhoff (Reference 22) using the full Breit-Pauli hamiltonian (solid lines) and the 1-electron 1-center effective spin-orbit operator (circles and crosses)

Figure 12. The potential energy curves for the ground states of AuH and AuCl obtained using a nonrelativistic (NR) and relativistic (R) ECP and a generalized valence bond wavefunction.

Figure 13. Geometrical and energetic parameters calculated by Hay (Reference 30) for Zeise's salt, and comparison with experimentally observed values (in parentheses).

Figure 14. Comparison of the Hartree-Fock valence orbitals with the valence pseudo-orbitals of the "linear-combination-of-atomic-orbitals" approach and the "shape consistent" approach for the case of the 3s orbital of silicon atom in the ^3P state.

Figure 15. Comparison of the all-electron potential energy curve for the Cl_2 molecule in the $X'\Sigma_g^+$ state (calculated with a generalized valence bond wavefunction) with the corresponding valence electron results using ECP's from three different approaches: the "shape-consistent" approach (Christiansen, Lee, and Pitzer; Reference 39), the old "linear-combination-of-atomic-orbitals" approach, and the "intermediate-fix" approach.

Figure 16. Comparison of the characteristics of the "charge accumulation" function of the Hartree-Fock 3s orbital of silicon atom, as a function of radial distance, with the "charge accumulation" function obtained from the valence pseudo-orbitals of the "shape-consistent" approach and the old "linear-combination-of-atomic-orbitals" approach.

Figure 17. Comparison of the characteristics of the Coulomb potential, as a function of radial distance, obtained from the density of the Hartree-Fock 3s orbital of silicon atom with the Coulomb potential obtained from the valence pseudo-orbitals of the "shape consistent" approach and the old "linear-combination-of-atomic-orbital" approach.

APPENDIX B

LISTING OF THE COMPUTER CODE THAT GENERATES THE NON-ZERO UNIQUE TERMS IN THE INTEGRAL FORMULAE OF THE ECP OVER CARTESIAN GAUSSIAN BASIS FUNCTIONS

```
      PROGRAM SHELL(INPUT,OUTPUT)
C
      DIMENSION LABL(4)
      DATA LABL/1HS,1HP,1HD,1HF/
C
      CALL ZTAB
      CALL FTAB
C
C...LOOP OVER SHELLS
      DO 240 NS=1,4
      DO 230 NSP=1,NS
C
      PRINT 400
C
C....LOOP OVER COMPONENTS OF THE SHELLS
      DO 220 LS=1,NS
      MSMAX=2*LS-1
      DO 210 MS=1,MSMAX,2
C
C
      DO 200 LSP=1,NSP
      MSPMAX=2*LSP-1
      DO 190 MSP=1,MSPMAX,2
C
      NX=(MS-1)/2
      NY=(2*LS-MS-1)/2
      NZ=NS-LS
C
      NXP=(MSP-1)/2
      NYP=(2*LSP-MSP-1)/2
      NZP=NSP-LSP
C
      PRINT 500,LABL(NS),LABL(NSP)
      PRINT 510,NS-1,LS-1,MS-LS,NX,NY,NZ,NSP-1,LSP-1,MSP-LSP,NXP,NYP,NZP
C
C
C...LOOP OVER THE TERMS IN A PARTICULAR INTEGRAL
      CALL INKIND(NS,LS,MS,NSP,LSP,MSP)
C
  190 CONTINUE
  200 CONTINUE
C
  210 CONTINUE
  220 CONTINUE
C
  230 CONTINUE
  240 CONTINUE
C
      STOP
C
  400 FORMAT(1H1)
  500 FORMAT(1H0,//,10X,A1,3X,A1,/)
  510 FORMAT(2X,2(5X,1H(,3I2,1H),1H/),1H(,3I2,1H))
      END
```

```
      FUNCTION DCO(L,M,KX,KY,KZ,LP,MP)
C...THIS ROUTINE EVALUATES THE ANGULAR MOMENTUM COUPLING CONSTANTS
      COMMON/FTABCM/FPQR(13,13,13)
      COMMON/ZTABCM/LMF(49),LML(49),ZLM(130),LMX(130),LMY(130),LMZ(130)
C
      ID=L*(L+1)-M+1
      IMN=LMF(ID)
      IMX=LML(ID)
C
      JD=LP*(LP+1)-MP+1
      JMN=LMF(JD)
      JMX=LML(JD)
C
      SUMI=0.0E0
      DO 20 I=IMN,IMX
      SUMJ=0.0E0
      DO 10 J=JMN,JMX
      JX=LMX(I)+KX+LMX(J)+1
      JY=LMY(I)+KY+LMY(J)+1
      JZ=LMZ(I)+KZ+LMZ(J)+1
   10 SUMJ=SUMJ + ZLM(J)*FPQR(JX,JY,JZ)
   20 SUMI=SUMI + ZLM(I)*SUMJ
C
      DCO=SUMI
      RETURN
       END
```

```
      FUNCTION ECO(KX,KY,KZ,L,M,KXP,KYP,KZP)
C
      COMMON/ZTABCM/LMF(49),LML(49),ZLM(130),LMX(130),LMY(130),LMZ(130)
      COMMON/FTABCM/FPQR(13,13,13)
C
      ID=L*(L+1)-M+1
      IMN=LMF(ID)
      IMX=LML(ID)
C
      SUM=0.0E0
      DO 10 I=IMN,IMX
      IX=KX+LMX(I)+KXP+1
      IY=KY+LMY(I)+KYP+1
      IZ=KZ+LMZ(I)+KZP+1
      SUM=SUM+ZLM(I)*FPQR(IX,IY,IZ)
   10 CONTINUE
C
      ECO=SUM
      RETURN
       END
```

```
      SUBROUTINE FTAB
C...THIS ROUTINE SETS UP A TABLE OF F-FUNCTION VALUES
C
      INTEGER P,Q,R
      COMMON/FTABCM/FPQR(13,13,13)
      DATA PI/3.1415926535898E0/
C
C...ZERO-OUT THE TABLE
      DO 30 P=1,13
      DO 20 Q=1,13
      DO 10 R=1,13
   10 FPQR(P,Q,R)=0.0E0
   20 CONTINUE
   30 CONTINUE
C
C...RECURSIVELY GENERATE THE NON-ZERO ENTRIES TO THE TABLE
      FPQR(1,1,1)=4.0E0*PI
      DO 80 P=1,13,2
      PP=P-1
      DO 70 Q=1,13,2
      QQ=Q-1
      DO 60 R=1,13,2
      RR=R-1
C
      IF (P.EQ.1) GO TO 40
      FPQR(P,Q,R)=(PP-1.0E0)*FPQR(P-2,Q,R)/(PP+QQ+RR+1.0E0)
      GO TO 60
   40 IF (Q.EQ.1) GO TO 50
      FPQR(P,Q,R)=(QQ-1.0E0)*FPQR(P,Q-2,R)/(PP+QQ+RR+1.0E0)
      GO TO 60
   50 IF (R.EQ.1) GO TO 60
      FPQR(P,Q,R)=(RR-1.0E0)*FPQR(P,Q,R-2)/(PP+QQ+RR+1.0E0)
C
   60 CONTINUE
   70 CONTINUE
   80 CONTINUE
C
      RETURN
       END
```

```
      SUBROUTINE ZTAB
C...THIS ROUTINE SETS UP THE REAL SPHERICAL HARMONICS IN THE FORM OF LINEAR
C...COMBINATIONS OF CARTESIAN PRODUCTS-(L,M)EL(L+1)-M+1
      COMMON/ZTABCM/LMF(49),LML(49),ZLM(130),LMX(130),LMY(130),LMZ(130)
C
      DATA FPI/12.566370614359E0/
      DATA LMF/1,2,3,4,5,7,8,10,11,12,14,16,18,20,22,23,25,28,30,34,36,
     X39,41,43,45,47,50,53,57,61,64,67,70,72,76,78,81,84,87,93,97,103,
     X106,110,113,116,120,124,127/
      DATA LML/1,2,3,4,6,7,9,10,11,13,15,17,19,21,22,24,27,29,33,35,38,
     X40,42,44,46,49,52,56,60,63,66,69,71,75,77,80,83,86,92,96,102,105,
     X109,112,115,119,123,126,130/
      DATA LMX/0,1,0,0,2,0,1,0,0,0,1,3,1,2,0,1,1,0,0,0,0,1,2,0,4,2,0,3,
     X1,2,0,0,2,1,1,0,0,0,0,0,1,1,2,0,3,1,5,3,1,0,2,4,3,1,1,3,2,0,2,0,1,
     X1,1,0,0,0,0,0,0,1,1,2,2,0,0,3,1,4,2,0,5,3,1,5,3,1,4,2,0,4,2,0,3,1,
     X1,3,2,0,2,0,2,0,1,1,1,0,0,0,0,0,0,0,0,1,1,1,2,0,2,0,3,1,3,1,4,2,0,6,
     X4,2,0/
      DATA LMY/0,0,0,1,0,2,0,0,0,1,1,0,2,0,2,0,0,0,0,0,1,1,1,1,3,0,2,4,0,
     X2,0,2,2,0,0,0,0,0,0,1,1,1,1,1,3,1,3,0,2,4,4,2,0,0,2,2,0,0,2,0,2,0,
     X0,0,0,0,0,1,1,1,1,1,1,1,3,3,1,3,1,3,5,1,3,5,0,2,4,0,2,4,0,2,4,0,2,
     X2,0,0,2,0,2,0,2,0,0,0,0,0,0,0,1,1,1,1,1,1,1,3,1,3,1,3,1,3,1,3,5,0,
     X2,4,6/
      DATA LMZ/0,0,1,0,0,0,1,2,0,1,0,0,0,1,1,2,0,3,1,2,0,1,0,0,0,0,0,1,
     X1,2,2,0,0,0,3,1,4,2,0,3,1,2,0,1,1,0,0,0,0,0,1,1,1,2,2,0,0,3,3,1,1,4,
     X2,0,5,3,1,4,2,0,3,1,2,0,2,0,1,1,0,0,0,0,0,0,1,1,1,2,2,2,0,0,0,3,3,
     X1,1,4,4,2,2,0,0,5,3,1,6,4,2,0,5,3,1,4,2,0,3,3,1,1,2,2,0,0,1,1,1,0,
     X0,0,0/
C
      ZLM(1)=SQRT(1.0E0/FPI)
      ZLM(2)=SQRT(3.0E0/FPI)
      ZLM(3)=ZLM(2)
      ZLM(4)=ZLM(2)
      ZLM(5)=SQRT(15.0E0/FPI)/2.0E0
      ZLM(6)=-ZLM(5)
      ZLM(7)=2.0E0*ZLM(5)
      ZLM(8)=3.0E0*SQRT(5.0E0/FPI)/2.0E0
      ZLM(9)=-ZLM(8)/3.0E0
      ZLM(10)=ZLM(7)
      ZLM(11)=ZLM(7)
      ZLM(12)=SQRT(35.0E0/(8.0E0*FPI))
      ZLM(13)=-3.0E0*ZLM(12)
      ZLM(14)=SQRT(105.0E0/(4.0E0*FPI))
      ZLM(15)=-ZLM(14)
      ZLM(16)=5.0E0*SQRT(21.0E0/(8.0E0*FPI))
      ZLM(17)=-ZLM(16)/5.0E0
      ZLM(18)=5.0E0*SQRT(7.0E0/FPI)/2.0E0
      ZLM(19)=-3.0E0*ZLM(18)/5.0E0
      ZLM(20)=ZLM(16)
      ZLM(21)=ZLM(17)
      ZLM(22)=2.0E0*ZLM(14)
      ZLM(23)=-ZLM(13)
      ZLM(24)=-ZLM(12)
      ZLM(25)=SQRT(315.0E0/(64.0E0*FPI))
      ZLM(26)=-6.0E0*ZLM(25)
      ZLM(27)=ZLM(25)
      ZLM(28)=SQRT(315.0E0/(8.0E0*FPI))
      ZLM(29)=-3.0E0*ZLM(28)
```

```
      TEMP=SQRT(45.0E0/FPI)/4.0E0
      ZLM(30)=7.0E0*TEMP
      ZLM(31)=-ZLM(30)
      ZLM(32)=TEMP
      ZLM(33)=-TEMP
      TEMP=SQRT(45.0E0/(8.0E0*FPI))
      ZLM(34)=7.0E0*TEMP
      ZLM(35)=-3.0E0*TEMP
      TEMP=SQRT(9.0E0/FPI)/8.0E0
      ZLM(36)=35.0E0*TEMP
      ZLM(37)=-30.0E0*TEMP
      ZLM(38)=3.0E0*TEMP
      ZLM(39)=ZLM(34)
      ZLM(40)=ZLM(35)
      TEMP=SQRT(45.0E0/(4.0E0*FPI))
      ZLM(41)=7.0E0*TEMP
      ZLM(42)=-TEMP
      ZLM(43)=-ZLM(29)
      ZLM(44)=-ZLM(28)
      ZLM(45)=SQRT(315.0E)/(4.0E0*FPI))
      ZLM(46)=-ZLM(45)
      ZLM(47)=SQRT(693.0E0/(128.0E0*FPI))
      ZLM(48)=-10.0E0*ZLM(47)
      ZLM(49)=5.0E0*ZLM(47)
      ZLM(50)=SQRT(3465.0E0/(64.0E0*FPI))
      ZLM(51)=-6.0E0*ZLM(50)
      ZLM(52)=ZLM(50)
      TEMP=SQRT(385.0E0/(128.0E0*FPI))
      ZLM(53)=9.0E0*TEMP
      ZLM(54)=-27.0E0*TEMP
      ZLM(55)=3.0E0*TEMP
      ZLM(56)=-TEMP
      TEMP=SQRT(1155.0E0/FPI)/4.0E0
      ZLM(57)=3.0E0*TEMP
      ZLM(58)=-ZLM(57)
      ZLM(59)=-TEMP
      ZLM(60)=+TEMP
      TEMP=SQRT(165.0E0/FPI)/8.0E0
      ZLM(61)=21.0E0*TEMP
      ZLM(62)=-14.0E0*TEMP
      ZLM(63)=TEMP
      TEMP=SQRT(11.0E)/FPI)/8.0E0
      ZLM(64)=63.0E0*TEMP
      ZLM(65)=-70.0E0*TEMP
      ZLM(66)=15.0E0*TEMP
      ZLM(67)=ZLM(61)
      ZLM(68)=ZLM(62)
      ZLM(69)=ZLM(63)
      TEMP=SQRT(1155.0E0/FPI)/2.0E0
      ZLM(70)=3.0E0*TEMP
      ZLM(71)=-TEMP
      ZLM(72)=-ZLM(54)
      ZLM(73)=-ZLM(55)
      ZLM(74)=-ZLM(53)
      ZLM(75)=-ZLM(56)
      ZLM(76)=SQRT(3465.0E0/FPI)/2.0E
      ZLM(77)=-ZLM(76)
```

```
      ZLM(78)=ZLM(49)
      ZLM(79)=ZLM(48)
      ZLM(80)=ZLM(47)
      TEMP=SQRT(3003.0E0/(512.0E0*FPI))
      ZLM(81)=6.0E0*TEMP
      ZLM(82)=-20.0E0*TEMP
      ZLM(83)=ZLM(81)
      ZLM(84)=SQRT(9009.0E0/(128.0E0*FPI))
      ZLM(85)=-10.0E0*ZLM(94)
      ZLM(86)=5.0E0*ZLM(84)
      TEMP=SQRT(819.0E0/(256.0E0*FPI))
      ZLM(87)=11.0E0*TEMP
      ZLM(88)=-66.0E0*TEMP
      ZLM(89)=ZLM(87)
      ZLM(90)=-TEMP
      ZLM(91)=6.0E0*TEMP
      ZLM(92)=-TEMP
      TEMP=SQRT(1365.0E0/(128.0E0*FPI))
      ZLM(93)=11.0E0*TEMP
      ZLM(94)=-33.0E0*TEMP
      ZLM(95)=9.0E0*TEMP
      ZLM(96)=-3.0E0*TEMP
      TEMP=SQRT(1365.0E0/(512.0E0*FPI))
      ZLM(97)=33.0E0*TEMP
      ZLM(98)=-ZLM(97)
      ZLM(99)=-18.0E0*TEMP
      ZLM(100)=+18.0E0*TEMP
      ZLM(101)=TEMP
      ZLM(102)=-TEMP
      TEMP=SQRT(273.0E0/FPI)/8.0E0
      ZLM(103)=33.0E0*TEMP
      ZLM(104)=-30.0E0*TEMP
      ZLM(105)=5.0E0*TEMP
      TEMP=SQRT(13.0E0/FPI)/16.0E0
      ZLM(106)=231.0E0*TEMP
      ZLM(107)=-315.0E0*TEMP
      ZLM(108)=105.0E0*TEMP
      ZLM(109)=-5.0E0*TEMP
      ZLM(110)=ZLM(103)
      ZLM(111)=ZLM(104)
      ZLM(112)=ZLM(105)
      TEMP=SQRT(1365.0E0/(128.0E0*FPI))
      ZLM(113)=33.0E0*TEMP
      ZLM(114)=-18.0E0*TEMP
      ZLM(115)=TEMP
      ZLM(116)=-ZLM(94)
      ZLM(117)=-ZLM(93)
      ZLM(118)=-ZLM(95)
      ZLM(119)=-ZLM(96)
      TEMP=SQRT(819.0E0/FPI)/4.0E0
      ZLM(120)=11.0E0*TEMP
      ZLM(121)=-ZLM(120)
      ZLM(122)=-TEMP
      ZLM(123)=TEMP
      ZLM(124)=ZLM(86)
      ZLM(125)=ZLM(85)
      ZLM(126)=ZLM(84)

      ZLM(127)=SQRT(3003.0E0/(512.0E0*FPI))
      ZLM(128)=-15.0E0*ZLM(127)
      ZLM(129)=-ZLM(128)
      ZLM(130)=-ZLM(127)
      RETURN
       END
```

```
      SUBROUTINE EXPAND(NS,LS,MS,L1,NT,NTP,NSP,LSP,MSP)
C...GENERATE THE TRANSLATION INDUCED EXPANSION TERMS FOR THE ECP INTEGRALS OF
C...THE FIRST KIND
C
      IFLAG=0
C
      LTMIN=MAXO(0,NT+LS-NS-1)+1
      LTMAX=MINO(LS-1,NT-1)+1
      DO 50 LT=LTMIN,LTMAX
      MTMIN=MAXO(-LT+1,MS-2*LS+LT)
      MTMAX=MINO(LT-1,MS-LT)
      MTMAX=MTMAX-MTMIN+1
      DO 40 MT=1,MTMAX,2
C
      NXT=(LT+MT+MTMIN-2)/2
      NYT=(LT-MT-MTMIN)/2
      NZT=NT-LT
C
C
      LTPMIN=MAXO(0,NTP+LSP-NSP-1)+1
      LTPMAX=MINO(LSP-1,NTP-1)+1
      DO 30 LTP=LTPMIN,LTPMAX
      MTPMIN=MAXO(-LTP+1,MSP-2*LSP+LTP)
      MTPMAX=MINO(LTP-1,MSP-LTP)
      MTPMAX=MTPMAX-MTPMIN+1
      DO 20 MTP=1,MTPMAX,2
C
      NXTP=(LTP+MTP+MTPMIN-2)/2
      NYTP=(LTP-MTP-MTPMIN)/2
      NZTP=NTP-LTP
C
C
      JFLAG=0
      M1MAX=2*L1-1
      DO 10 M1=1,M1MAX
C
      TEMP=ECO(NXT,NYT,NZT,L1-1,M1-L1,NXTP,NYTP,NZTP)
      IF (ABS(TEMP).LT.1.0E-10) GO TO 10
C
      IFLAG=IFLAG+1
      IF (IFLAG.GT.1) GO TO 5
      PRINT 520,L1-1,NT-1,NTP-1
    5 CONTINUE
C
      JFLAG=JFLAG+1
      IF (JFLAG.GT.1) GO TO 7
      PRINT 530,NT-1,LT-1,MT+MTMIN-1,NXT,NYT,NZT,NTP-1,LTP-1,
     1          MTP+MTPMIN-1,NXTP,NYTP,NZTP
    7 CONTINUE
C
      PRINT 540,M1-L1,TEMP
C
   10 CONTINUE
C
   20 CONTINUE
   30 CONTINUE
C


   40 CONTINUE
   50 CONTINUE
C
      RETURN
C
  520 FORMAT(1HO,10X,3HL1=,I2,2X,3HN1=,I2,2X,3HN2=,I2)
  530 FORMAT(15X,5X,1H(,3I2,3H)/(,3I2,1H),32X,3X,1H(,3I2,3H)/(,3I2,1H))
  540 FORMAT(42X,2HM=,I2,3X,E15.8)
      END
```

```
      SUBROUTINE INKIND(NS,LS,MS,NSP,LSP,MSP)
C...LOOP OVER THE TERMS IN THE ECP INTEGRALS OF THE FIRST KIND
C
      L1MAX=NS+NSP-1
      DO 30 L1=1,L1MAX
C
      DO 20 NT=1,NS
C
      DO 10 NTP=1,NSP
C
C
C...GENERATE THE TRANSLATION INDUCED EXPANSION TERMS
      CALL EXPAND(NS,LS,MS,L1,NT,NTP,NSP,LSP,MSP)
C
   10 CONTINUE
   20 CONTINUE
   30 CONTINUE
C
      RETURN
C
       END
```

```
      SUBROUTINE EXPAND(NS,LS,MS,L,L1,L2,NT,NTP,NSP,LSP,MSP)
C...GENERATE THE TRANSLATION INDUCED EXPANSION TERMS FOR THE ESP INTEGRALS OF
C...OF THE SECOND KIND
C
      IFLAG=0
C
      LTMIN=MAX0(0,NT+LS-NS-1)+1
      LTMAX=MIN0(LS-1,NT-1)+1
      DO 70 LT=LTMIN,LTMAX
      MTMIN=MAX0(-LT+1,MS-2*LS+LT)
      MTMAX=MIN0(LT-1,MS-LT)
      MTMAX=MTMAX-MTMIN+1
      DO 60 MT=1,MTMAX,2
C
      NXT=(LT+MT+MTMIN-2)/2
      NYT=(LT-MT-MTMIN)/2
      NZT=NT-LT
C
C
      LTPMIN=MAX0(0,NTP+LSP-NSP-1)+1
      LTPMAX=MIN0(LSP-1,NTP-1)+1
      DO 50 LTP=LTPMIN,LTPMAX
      MTPMIN=MAX0(-LTP+1,MSP-2*LSP+LTP)
      MTPMAX=MIN0(LTP-1,MSP-LTP)
      MTPMAX=MTPMAX-MTPMIN+1
      DO 40 MTP=1,MTPMAX,2
C
      NXTP=(LTP+MTP+MTPMIN-2)/2
      NYTP=(LTP-MTP-MTPMIN)/2
      NZTP=NTP-LTP
C
C
      JFLAG=0
C
      M1MAX=2*L1-1
      DO 30 M1=1,M1MAX
      M2MAX=2*L2-1
      DO 20 M2=1,M2MAX
      MMAX=2*L-1
      DO 10 M=1,MMAX
C
      TEMP1=GCO(L1-1,M1-L1,NXT,NYT,NZT,L-1,M-L)
      TEMP2=GCO(L2-1,M2-L2,NXTP,NYTP,NZTP,L-1,M-L)
      IF ((ABS(TEMP1).LT.1.0E-10).OR.(ABS(TEMP2).LT.1.0E-10)) GO TO 10
C
      IFLAG=IFLAG+1
      IF (IFLAG.GT.1) GO TO 5
      PRINT 400,L-1,L1-1,L2-1,NT-1,NTP-1
    5 CONTINUE
C
      JFLAG=JFLAG+1
      IF (JFLAG.GT.1) GO TO 7
      PRINT 500,NT-1,LT-1,MT+MTMIN-1,NXT,NYT,NZT,NTP-1,LTP-1,
     1          MTP+MTPMIN-1,NXTP,NYTP,NZTP
    7 CONTINUE
C
      PRINT 510,M1-L1,M2-L2,M-L,TEMP1,TEMP2
C
   10 CONTINUE
   20 CONTINUE
   30 CONTINUE
C
C
   40 CONTINUE
   50 CONTINUE
C
C
   60 CONTINUE
   70 CONTINUE
C
      RETURN
C
  400 FORMAT(1H0,10X,2HL=,I2,2X,3HL1=,I2,2X,3HL2=,I2,2X,3HN1=,I2,2X,
     1       3HN2=,I2)
  500 FORMAT(15X,5X,1H(,3I2,3H)/(,3I2,1H),32X,3X,1H(,3I2,3H)/(,3I2,1H))
  510 FORMAT(30X,3HM1=,I2,2X,3HM2=,I2,2X,2HM=,I2,3X,E15.8,3X,E15.8)
      END
```

```
      SUBROUTINE INKIND(NS,LS,MS,NSP,LSP,MSP)
C...LOOP OVER THE TERMS IN THE ECP INTEGRALS OF THE SECOND KIND
C
      DO 50 L=1,4
C
      L1MAX=L+NS-1
      DO 40 L1=1,L1MAX
C
      L2MAX=L+NSP-1
      DO 30 L2=1,L2MAX
C
      DO 20 NT=1,NS
C
      DO 10 NTP=1,NSP
C
      CALL EXPAND(NS,LS,MS,L,L1,L2,NT,NTP,NSP,LSP,MSP)
C
   10 CONTINUE
   20 CONTINUE
   30 CONTINUE
   40 CONTINUE
   50 CONTINUE
C
      RETURN
C
       END
```